Jül-4394

Institute of Energy and Climate Research
Stratosphere (IEK-7)

Stratospheric Ozone Depletion: Analysis of Heterogeneous Chemistry in the Antarctic

Abdul Mannan Zafar

Mitglied der Helmholtz-Gemeinschaft

JÜLICH
FORSCHUNGSZENTRUM

Stratospheric Ozone Depletion: Analysis of Heterogeneous Chemistry in the Antarctic

Abdul Mannan Zafar

Berichte des Forschungszentrums Jülich; 4394
ISSN 0944-2952
Institute of Energy and Climate Research
Stratosphere (IEK-7)
Jül-4394

DE 17 (Master, TU Darmstadt, 2016)

Vollständig frei verfügbar über das Publikationsportal des Forschungszentrums Jülich (JuSER)
unter www.fz-juelich.de/zb/openaccess

Forschungszentrum Jülich GmbH
Zentralbibliothek, Verlag
52425 Jülich
Tel.: +49 2461 61-5220
Fax: +49 2461 61-6103
E-Mail: zb-publikation@fz-juelich.de
www.fz-juelich.de/zb

Stratospheric Ozone Depletion: Analysis of Heterogeneous Chemistry in the Antarctic

Abdul Mannan Zafar

Jülich, May 2016

This report constitutes the Master-Thesis of Abdul Mannan Zafar (Matr.-Nr.: 2735852) at the Technische Universiät Darmstadt. The thesis was supervised by Prof. Dr. Martin Ebert (TU Darmstadt) and Dr. Rolf Müller (Forschungszentrum Jülich) and was accepted at the TU Darmstadt in May 2016. This version printed in the series “Berichte des Forschungszentrums Jülich” was subject to minor copy editing by Rolf Müller and Jens-Uwe Grooß.

Keep your dreams alive. Understand to achieve anything
requires faith and belief in yourself,
vision, hard work, determination, and dedication.
Remember all things are
possible for those who believe.

I dedicate my efforts to my beloved
parents who always supported me

اپنی مہنت اور لگن کی مدد سے ھر کام
پایا تکمل تک پھنچیا جا سکتا ہے۔لگن
کی مدد سے خواب مکمل۔ پختا عزم
کی امئد لگایی جا سکتی ھے۔

Table of Contents

List of Figures

List of Tables

Acknowledgements

This work was carried out during my stay in Germany, at the Technical University of Darmstadt and at the Institute of Energy and Climate Research (IEK-7), Forschungszentrum Jülich.

I owe my deepest gratitude to my supervisor in Environmental Geology at Technical University of Darmstadt, Prof. Dr. Martin Ebert. Without his continuous optimism concerning this work, enthusiasm, encouragement and support this study would hardly have been completed.

I also express my warmest gratitude to my other supervisor Dr. Rolf Müller, who suggested this topic to me. His guidance into the world of atmospheric science and supervision in ozone depletion have been essential during this work.

I am deeply grateful to Dr. Jens-Uwe Grooß who supported and helped me to run the model successfully, without his support carrying out this work would not have been possible.

I am thankful to my parents, who pray for my success and support me through difficult times.

Abstract

In spite of the success of the Montreal protocol and its amendments and adjustments in reducing the stratospheric chlorine loading, due to the long atmospheric lifetime of chlorine source gases, the Antarctic ozone hole will continue to occur for decades (WMO, 2014). The ozone hole arises from ozone destruction driven by elevated levels of ozone destroying ("active") chlorine in Antarctic spring. The established picture of the development of the ozone hole is that high levels of active chlorine are maintained in Antarctic spring by a competition between chlorine deactivation through gas-phase formation of $ClONO_2$ and HCl and activation of $ClONO_2$ and HCl by heterogeneous reactions (Solomon et al., 2014, 2015). In the core of vortex for ozone hole conditions in the lower stratosphere (i.e. 16-18 km or 100-70 hPa) formation of $ClONO_2$ is of minor importance and the formation of HCl by reaction of Cl with CH_4 and CH_2O cannot lead to deactivation because it is balanced by immediate reactivation in effective reaction cycles involving the heterogeneous reaction HCl+HOCl. For the (observed) complete activation of stratospheric chlorine the production of HOCl via HO_2 + ClO, with the HO_2 resulting from CH_2O photolysis, is essential. These results are key for assessing the impact of changes of the future stratospheric composition on the recovery of Antarctic ozone. Our simulations indicate that future increased methane concentrations will not lead to enhanced chlorine deactivation and that extreme ozone destruction to levels below ≈ 0.1 ppm will occur until mid-century. Besides the reactions involved in the activation and rapid deactivation of chlorine are analysed here thoroughly.

1 Introduction

1.1 Ozone in the atmosphere

An ozone molecule contains three atoms of oxygen O^{16} bound together as shown in figure 1.1a. Most atmospheric ozone is present at a certain distance from the Earth's surface. Normally, the atmosphere is divided into four major layers named Troposphere, Stratosphere, Mesosphere and Thermosphere. Concentration of ozone varies from layer to layer and with altitude under different conditions of temperature and pressure. Ozone molecules are much less abundant in the atmosphere than oxygen. 90% of

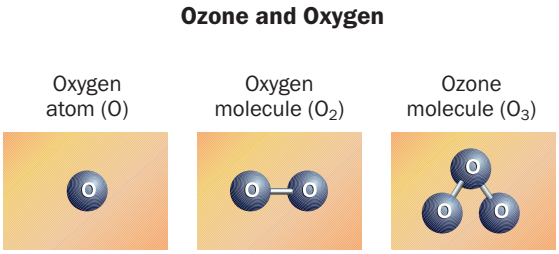

(a) Representation of oxygen atom, oxygen molecule O_2 and ozone molecule. Figure from (WMO, 2014)

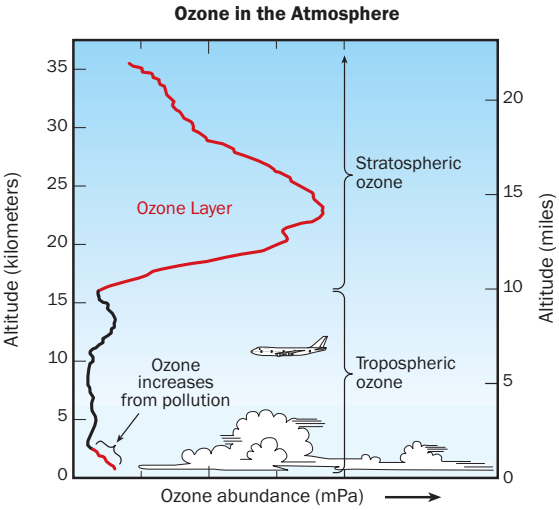

(b) Profile illustrating location of ozone in the atmosphere. The vertical thickness varies with the regional and seasonal variations. The ozone increase near to surface of Earth is due to human activities causing increase in pollution (WMO, 2014).

Figure 1.1: Structure of Ozone and Ozone Profile

ozone is found in the stratosphere and the remaining 10% is found in the troposphere. The stratospheric ozone layer exists in the atmosphere from the Earth's surface at 15-

20 kilometres in altitude (see figure 1.1b). Concentrations of ozone molecules are few thousands in billions of air molecules, where air molecules contain oxygen by 21% and nitrogen by 78% approximately. The vertical distribution of ozone in the atmosphere is illustrated in figure1.1b. Figure1.1b gives an idea for the tropospheric and stratospheric ozone layer in accordance with their corresponding altitudes. Ozone molecules in the stratosphere and troposphere are in gaseous form and if all the ozone molecules were compressed in the form of layer of pure ozone at standard conditions, this layer will have an average thickness of about 3 mm. However, this thin ozone layer is protecting all life on Earth from dangerous solar UV radiation.
Ozone is formed naturally in the stratosphere under the influence of sunlight, which dissociates oxygen molecules to oxygen atoms. The oxygen atom reacts with an oxygen molecule in the stratosphere to form an ozone molecule and this reaction continues in the presence of solar radiation. The largest ozone production occurs in the tropical stratosphere. The factors related to chemistry that support the process of ozone destruction will be discussed in the next chapters in detail.

1.2 Ozone measuring techniques

Since ozone is present in the atmosphere in gaseous phase, there are different methods to measure ozone. There are two main principles to measure ozone, local and remote. A local measurement is based on the direct input of air in the measuring instrument which detects ozone by its absorption of ultraviolet light, by passing of electrical current or light produced in a chemical reaction. The most common approach of the local measuring technique is an ozonesonde, which is a lightweight instrument with ozone measuring modules and carried by small balloons up in the air. The balloon can lift up enough to reach the stratospheric layer. Other local measuring instruments are connected to research aircraft based on optical or chemical detection schemes (e.g. Zahn et al., 2012). Some of the instruments are connected with commercial aircraft (Petzold et al., 2015).
Remote sensing measurements are carried out at larger distances from the air mass that contains the ozone. Remote sensing instruments measure total ozone amounts and altitude distributions of ozone globally. The remote measurements of ozone utilise unique absorption properties of UV radiation. Satellites are being used to measure ozone by UV radiation reflected back from the atmosphere and from the surface of the Earth on daily basis. Another method to measure ozone is by lasers, which send signals from

ground stations. These laser instruments can also be installed in research aircraft to detect ozone in the atmosphere along the laser light path (WMO, 2014). Other instruments to measure ozone from the ground based meteorological stations, these stations use ground based detectors which detect the small changes in the UV radiations infiltrating from the atmosphere to reach the surface of the Earth. However, some other instruments are used to measure ozone which absorbs infrared or visible radiation or its emission of microwave or infrared radiation. And mostly, these emission measurements are beneficial for providing remote ozone measurements at night, which is peculiar for sampling polar regions especially they collect data during the polar night when polar region is dark (WMO, 2014).

1.3 Unit of ozone measurements

The unit of ozone column is Dobson Unit (DU), named after the scientist who invented a spectrograph to measure ozone in 1924 for the first time, and his instrument was able to measure for extending time periods (Dobson and Harrison, 1926). The total thickness of ozone, if represented as a column of air is measured in Dobson Units (DU), where one Dobson unit is equal to $2.687 \cdot 10^{16}$ ozone molecules per square centimetre whereas, $1\mathrm{DU/km} \approx 3.717 \cdot 10^{12}$ molecules per cubic centimetre (Müller, 2012). Most of the time in atmospheric chemistry, the suitable way of expressing the amount of trace gases in gaseous phase is to represent as the ratio of number of moles to the number of moles of air which is known as mole fraction. This way of expression is termed as part per million (ppm), part per billion (ppb), and part per trillion (ppt) (Müller, 2012). Many times in this thesis the term which denotes the unit of ozone will be in ppmv or ppbv. The term ppmv denotes part per million by volume and part per billion by volume as ppbv; for an ideal gas mole fraction and volume mixing ratio are identical (Müller, 2012).

1.4 Ozone depletion: a global issue

The ozone hole is considered as a result of human produced CFCs which were traced in the air samples collected for the first time in the 1970's (Lovelock et al., 1973). Molina and Rowland (1974) were the first who published the role of CFCs in the stratosphere causing a disturbance in the stratosphere driven by chlorine at an altitude of approximately 40 kilometres, which could affect ozone. They figured out the ef-

fective role of chlorine that was depleting ozone with the increasing concentration of chlorine. Since then, the stratosphere became a sensitive issue for ozone depletion because most of the ozone is present in the stratosphere. In the mean while, supporting the theory from Molina and Rowland (1974), Crutzen (1974) presented the role of CF_2Cl_2 and $CFCl_3$ as main CFCs, suggesting ozone loss within 30 km altitude in stratosphere, no one did foresee the ozone hole by that time. Today it is confirmed that the main anthropogenic halogen compounds play the central role for ozone depletion. Several further compounds are being listed as ozone depleting substances containing chlorine and bromine, which are: methyl chloroform (CH_3Cl_3), carbon tetrachloride (CCl_4), halon-1211 (CF_2ClBr), halon-1301 (CF_3Br), halon-2402, CF_2BrCF_2Br, and CH_3Br (Montzka, 2012). After the ozone hole was discovered by Farman et al. (1985), the chemical reactions proceeding in the atmosphere have been studied more in depth (Solomon, 1999). A representation of important chemical species has been reported in scientific assessment of ozone depletion (WMO, 2014).

In figure 1.2, chemical species like nitric acid (HNO_3), hydrogen chloride (HCl) and chlorine monoxide (ClO) have been shown for 2008 during fall and late winter season. The data are collected from satellites, which can give daily plots of these chemical species. Both measurements for fall and late winter season are taken at an altitude of 18-kilometres. One thing is clear in the figure 1.2, temperature, HCl and ClO plays a vital role in ozone hole depletion. In fall season, temperature is moderate, amount of HNO_3 is high including HCl while the amount of ClO is quite low. Ozone is normally high in these conditions. In late winter, under sunlight condition, the concentration of HCl reduces dramatically and the ClO concentration adjacently increases and at the same time, HNO_3 is partly removed by gravitational settling of polar stratospheric clouds (PSC) particles and reduced to a low amount. High ClO concentrations have a great impact on ozone loss, which is clearly evident in figure 1.2. This figure indicates the importance of chlorine for polar ozone loss in the atmosphere, where the lower HCl and higher ClO concentrations are varying with season and temperature. In this study, heterogeneous chemistry involved in the stratosphere will be discussed in detail and the processes involved in ozone depletion will be investigated.

1.5 Antarctic ozone hole

In 1985, at the British Antarctic Survey station at Halley, extremely low total ozone column values were reported in Antarctic spring (Farman et al., 1985; Jones and Shank-

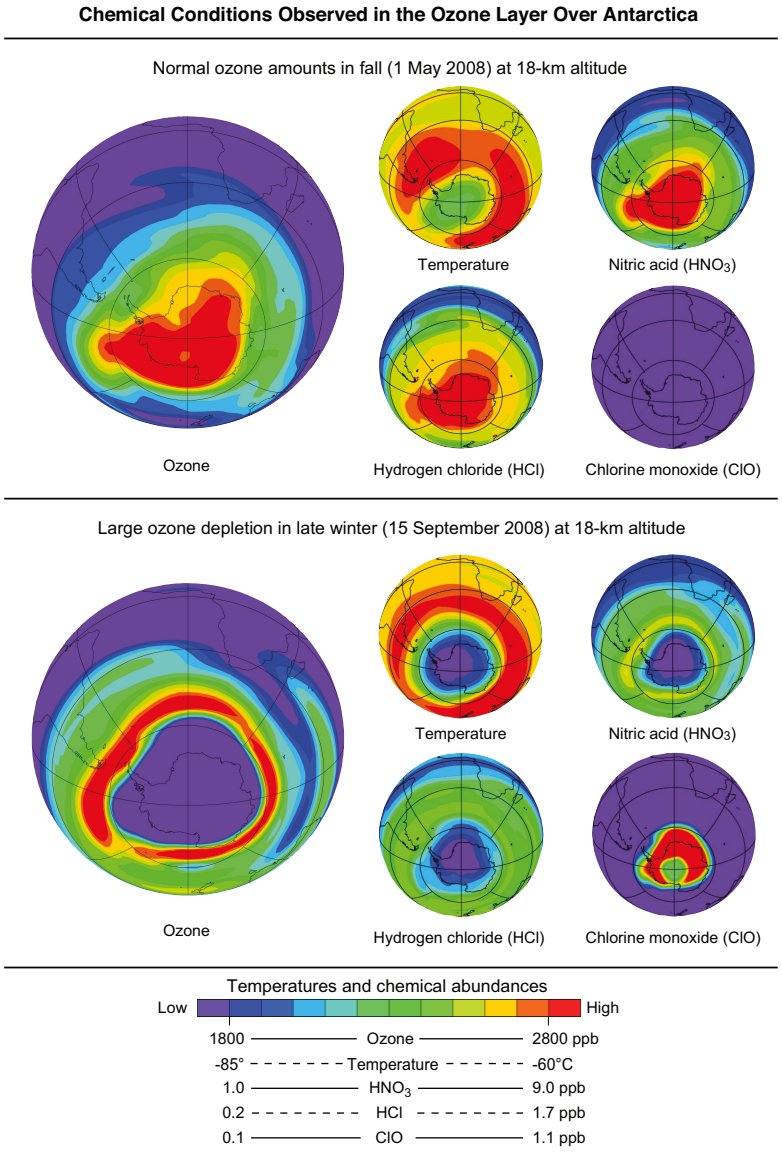

Figure 1.2: Chemical conditions observed in 2008 for fall (1 May 2008) and late winter (15 September 2008) season over Antarctica (WMO, 2014).

lin, 1995). This phenomenon of lowest total ozone values is known as the "Antarctic Ozone Hole" (Stolarski et al., 1986; Solomon, 1999; Müller, 2009). It is a clear example of human activities resulting in atmospheric change due to CFCs emissions. Satellite measurements confirmed the existence of the ozone hole over the entire Antarctic continent (Stolarski et al., 1986). A satellite measurement of total ozone on 14 September

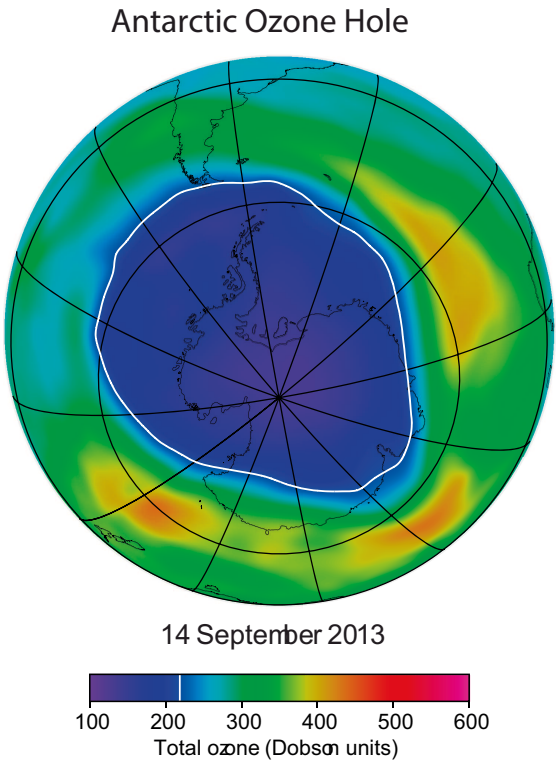

Figure 1.3: Antarctic Ozone hole in September 2013 (WMO, 2014).

2013, is shown in figure1.3. The dark blue region indicates the lower total ozone values over the entire Antarctic continent, which represents the ozone hole, which appears in every spring. Minimum values of total ozone inside the ozone hole are about 100 DU while for unperturbed conditions in springtime season the total ozone value would be in the range of 350 DU or larger. The term ozone hole was first suggested by Stolarski et al. (1986). Ozone measurements have been performed to analyse the ozone hole and they corroborated a significant difference in the ozone mixing ratios, typically lower partial pressures in mid-winter and spring (Solomon, 1999; Müller, 2009, 2012). Satellite measurements allowed more details about the vertical ozone distribution and chemical ozone loss in the ozone hole to be detected. Measurements of ozone mixing ratios lower than 0.1 ppm are typically not possible with satellites. Here ozonesonde observations are more reliable to access some unique information which can give insight on the

ozone layer recovery (Solomon et al., 2005a,b). While chemical destruction of ozone

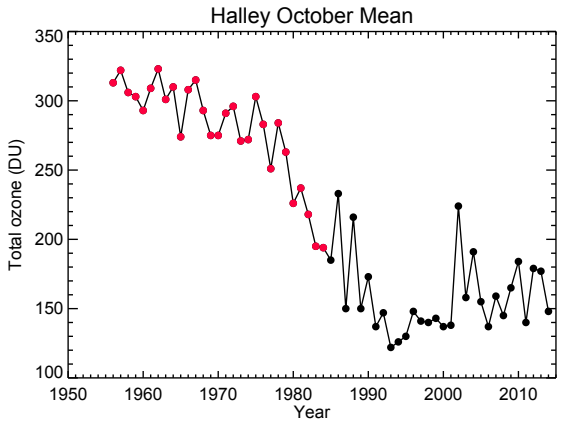

Figure 1.4: October mean values at Halley Station; updated from Müller (2010).

plays a vital role in the appearance of the ozone hole, dynamical processes also contribute to the formation. In fall, the polar vortex is formed over Antarctica and isolates the polar stratosphere lowering the temperature of the stratosphere and thus creating a thermal contrast between polar and mid-latitude air (Müller, 2012). The cooler air descends, and mid-latitude air travels poleward and a strong jet stream of air forms. And because of this wind jet, the Antarctic polar vortex is isolated from the mid-latitude stratosphere (Schoeberl and Hartmann, 1991). If there were no vortex isolation, mixing with mid-latitude air would make it difficult to maintain low temperatures and a disturbed chlorine chemistry as required for the chemical destruction of ozone (Solomon, 1999; Müller, 2012). Figure 1.4 represents the total column ozone measurements starting in the mid 1950's from Dobson spectrometer at Halley, Antarctica. The red dots indicated in figure 1.4 are data points published by Farman et al. (1985). The remaining data points are presented by Jones and Shanklin (1995) to the year 2009. The low ozone column values already concerned Farman et al. (1985) when he published the data in 1985 and they concluded that chlorine chemistry should be responsible for the observed low ozone values. In the late 1980's, the Montreal Protocol treaty was signed to control the emission of CFCs in the atmosphere.

1.5.1 South pole Ozone sonde observation

Figure 1.5 shows the South pole station ozone measurements at 70 hPa of winter and spring season taken from the year 1990 to 2010. In this study, we will investigate polar ozone chemistry in a box model environment, where an air parcel follows a trajectory

(see Chapter 3 below for details). The trajectory, we used in the standard run intersects very low ozone sonde observations at South pole. The ozone sonde observations are plotted on a log scale y-axis. The behaviour of the ozone sonde observations is similar to our trajectory model results. The ozone sonde observations are plotted for the years 1990-1999 in blue diamond shape, for the years 2000-2004 values in red dots and for the years 2005-2010 in green triangles. Throughout the years from 1990-2010 very low ozone values $\approx$ 10 ppbv were observed in early October. Figure 1.5 depicts the ozone hole period which usually occurs at South pole during the month of October every year. Very low ozone values are observed in October. The observations of the extremely low

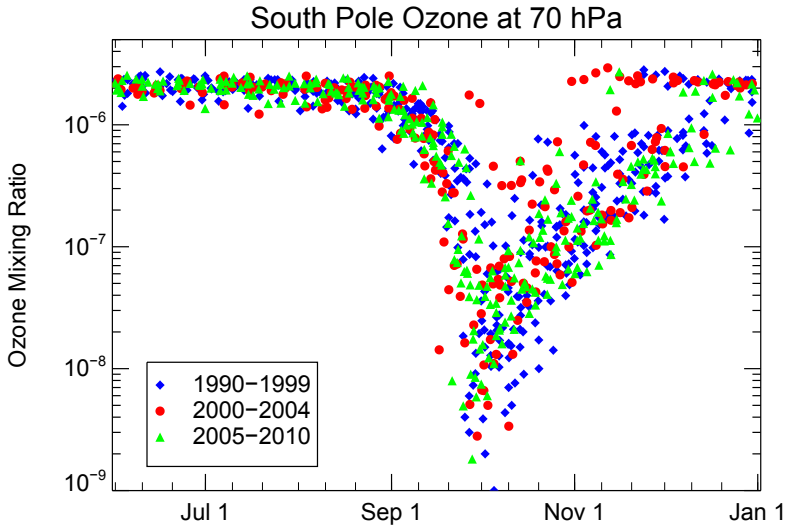

Figure 1.5: Ozone sonde observations at 70 hPa at South pole station in late winter and spring from the year 1990-2010. Figure taken from the study of Grooß et al. (2011) updated from the study of Solomon et al. (2005a).

ozone values in the core of the Antarctic vortex constitute part of the motivation for conducting the model studies presented below.

1.6 Montreal Protocol

An international treaty in 1987 under the influence of United Nations Environmental Programme (UNEP) was signed to take the initiative concerning the ozone hole and ozone depleting substances. The main agenda of Montreal Protocol was to control the emissions of ozone depleting substances (ODS) (UNEP, 1987). And this treaty came into act in 1989. Since then, CFC production and usage was reduced because CFCs constituted the largest source of chlorine concentration in the stratosphere. The impact

of Montreal Protocol on the long term changes of ODS abundances can be deduced from equivalent effective stratospheric chlorine (EESC). EESC is calculated based on chlorine and bromine present in the atmosphere which is the fundamental source of ozone destruction in the stratosphere (Daniel et al., 1996). The long term changes in EESC at global level are shown in figure1.6. Models indicate that if there were no protocol the chlorine would strongly increase resulting in a substantial reductions in total ozone between 1990 and 2010 (Newman et al., 2009). Figure1.6 showing the effect of equivalent effective stratospheric chlorine for mid-latitude including following cases: No Protocol provisions, Provision of original 1987 Montreal Protocol, Zero emissions of ODSs starting in 2011. The city names other than Montreal displayed in the figure1.6 represent the year and where the amendments and adjustments were modified in comparison to the original Montreal Protocol treaty. Methyl chloride is the most abundant

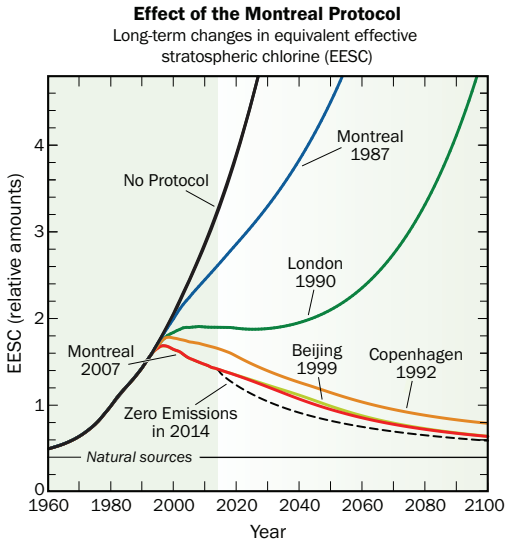

Figure 1.6: Significance of the Montreal Protocol and Amendments (WMO, 2014)

naturally emitted chlorine gas. Methyl chloride is present in the troposphere globally averaged concentration of about 550 ppt and responsible for 16% of chlorine loading in stratosphere (WMO, 2014). At the end of this century, when CFCs will likely be reduced to minimum values, the large contribution of chlorine in the stratosphere would be from methyl chloride (WMO, 2014; Müller, 2012). The halogen source gases in the atmosphere lead to stratospheric ozone depletion. The breakdown process of halogen source gases (e.g. CFCs) peaks in the upper stratosphere because of high energy solar radiation at those altitude. In this way chlorine atoms from the source gases are converted into reservoir species, mostly HCl and $ClONO_2$. These reservoir species do not destroy ozone directly, however if they are converted into active form they deplete

ozone. In figure1.7, the year 1980 is used as a reference for an undisturbed ozone layer.

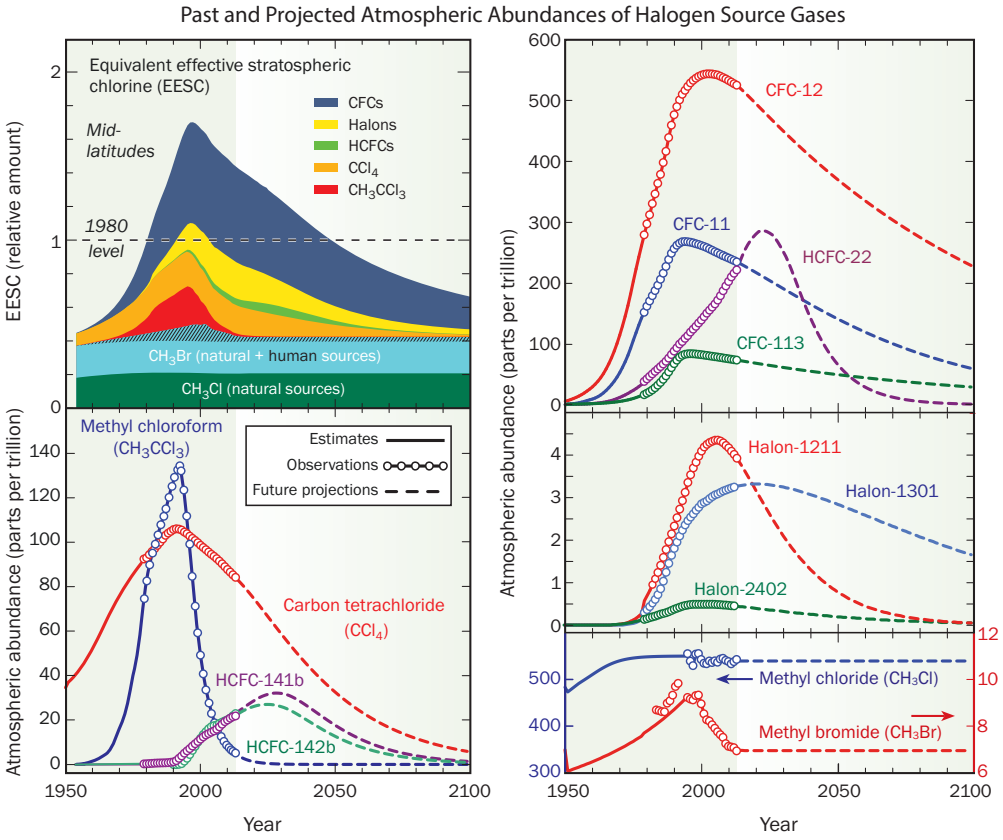

Figure 1.7: Halogen source gases time line distribution from 1950 to 2100 (WMO, 2014).

The rise of equivalent effective stratospheric chlorine in the 20th century has slowed down and reversed as compared to last two decades of the 19th century where the EESC values reached a maximum. Values are shown in figure1.7 depending upon halogen source gas abundances obtained from measurements, historical estimates of abundances and predictions of future abundances. The return of HCFCs values back to 1980 is estimated in 2065 in polar regions (WMO, 2014). EESC levels as shown in figure1.7 will return back to 1980 level in 2050. Because of the success of Montreal Protocol (UNEP, 1987) it is estimated that ODSs concentration and ozone hole recovery is expected by the end of this century. The concentration of HCFCs which are alternatives of CFCs will continue to increase for several years and methyl chloride is found naturally and is abundant in the atmosphere, therefore it is not regulated in the Montreal Protocol.

1.7 Scope of this study

The agenda of this study is to investigate heterogeneous chemistry in stratosphere, which is important to analyse the effect of chemical species and active chlorine in the stratosphere. For heterogeneous and gas phase chemistry different sensitivity analyses have been accomplished using the Chemical Lagrangian Model of the Stratosphere (CLaMS). Different cases have been run in the model to check the sensitivity on ozone depletion and the effect on chlorine activation and deactivation process. The main focus is to figure out the important chemical reactions taking place in spring season over polar stratospheric regions. Furthermore, the behaviour of chemical species due to reaction on polar stratospheric clouds, liquid surfaces, NAT and ice particles will be discussed. Moreover, the main theme of discussion is about the HCl and ClO_x behaviour; according to Grooß et al. (2011) mixing ratios of HCl rises up abruptly and similarly ClO_x drops down at the same time in early October, when extremely low ozone mixing ratios are observed. The mechanism behind HCl and ClO_x will be identified in this study, and will be explained in detail. The activation phase of chlorine is modelled and will be discussed in the next sections. These processes have been tested in the Chemical Lagrangian Model of the Stratosphere (CLaMS) with different assumptions for the chlorine activation and deactivation. The effect of photolysis on gas phase chemistry will be emphasised. Temperature variations and reaction rates will be used to distinguish the most important chemical reactions involving in the ozone depletion. Ozone depletion involves many aspects from heterogeneous chemistry, gas phase chemistry, air and wind dynamics, effect of greenhouse gases in lowering the stratospheric temperature and effect of the Brewer-Dobson circulation on ODSs. The impact of low concentrations of $ClONO_2$ in polar night (because of lower solar elevation, large solar zenith angle) on the development of HCl will be investigated. The role of HO_2 and OH will be synthesised in a sensitivity analysis to clarify, which chemical species is most relevant to deplete ozone. It is already known that, in the beginning of September, chlorine is activated that cause ozone depletion (Solomon, 1999; Müller and Crutzen, 1994), but the question remains unanswered, what causes the change of HCl that is a reservoir source to ClO_x conversion during the spring season (in the month of September). Different hypotheses are presented in this case, which is described in the next sections.

2 Motivation

The inspiration to conduct this study is to answer open questions in ozone depletion, which so far is not being completely understood. The role of $ClONO_2$ in stratospheric chemistry needs to be identified and its heterogeneous effect on surfaces like liquid, nitric acid trihydrate (NAT) and ice. So far, it is well understood that low temperatures in polar regions play a key role in causing ozone depletion. However, the role of HOCl in heterogeneous chemistry requires some more study. In this thesis, the main focus is to demonstrate that HOCl reacts at much faster rate than $ClONO_2$ to deplete ozone during Antarctic spring. The HO_x family components OH and HO_2, react to produce major components for heterogeneous chlorine activation, for instance $ClONO_2$ and HOCl respectively. Crutzen et al. (1992), pointed out importance of the methane oxidation in gaseous phase and the heterogeneous reaction $HOCl + HCl$. However, the exact chemical pathways to the observed complete chlorine activation are not understood. This study aims at making progress regarding these issues by analysing these chemical mechanisms in a series of box model calculations using the CLaMS model.

2.1 Background

2.1.1 Importance of heterogeneous reactions in ozone depletion

Heterogeneous chemistry is a key process in ozone depletion, it activates chlorine which in turn causes observed ozone depletion in Antarctic polar spring (Solomon et al., 1986; Solomon, 1999; Müller and Crutzen, 1994). The main focus of the present study is to analyse the mechanism behind the chlorine activation from reservoir species HCl and $ClONO_2$, the phenomenon involving in the conversion of reservoir species HCl into active chlorine ClO. The observation of low ozone mixing ratios and strongly enhanced ClO mixing ratios in the Antarctic stratosphere under "ozone hole" conditions was reported by Anderson et al. (1991). The chemical mechanism of ozone depletion

by active chlorine under such conditions was first put forward by Molina and Molina (1987).

$$\begin{aligned} ClO + ClO + M &\rightarrow Cl_2O_2 + M && \text{(R1)} \\ Cl_2O_2 + h\nu &\rightarrow Cl + ClOO && \text{(R2)} \\ ClOO + M &\rightarrow Cl + O_2 + M && \text{(R3)} \\ Cl + O_3 &\rightarrow ClO + O_2 \quad (2\times) && \text{(R4)} \\ \text{Net CR1}: \quad 2O_3 &\rightarrow 3O_2 && \text{(R5)} \end{aligned}$$

For the details of the above presented cycle (see 2.2.1). The hypothesis of reservoir species that is $ClONO_2$ and HCl reacting with each other producing active chlorine on NAT (Nitric acid trihydrate) or ice particles was presented by Solomon et al. (1986) and Tolbert et al. (1988):

$$ClONO_2 + HCl \rightarrow Cl_2 + HNO_3 \quad (\text{solid}) \tag{R6}$$

$$Cl_2 + h\nu \rightarrow 2Cl \tag{R7}$$

Later on, the importance of ClO cycle (CR1) which is also known as Dimer-cycle will be discussed here that how activated chlorine reacts in a different reactions to deplete ozone. Normally, the initial concentration of $ClONO_2$ is less than HCl, and the amount of Cl_2 being produced in polar night is less due to limited availability of $ClONO_2$. The reservoir species $ClONO_2$ is formed when an adequate amount of ClO and NO_2 is present. During polar night conditions, most of the NO_x is converted into N_2O_5, hence resulting in more HNO_3 by heterogeneous reactions on sulphate aerosol (Hanson and Ravishankara, 1991; Crutzen et al., 1992). In polar night conditions, photolysis of Cl_2 will not take place, which results in no ClO production resulting in no $ClONO_2$. Similarly, under sunlight conditions, through the photolysis of HNO_3 or its reaction with OH, conversion of activated chlorine ClO_x to inactivated chlorine i.e. $ClONO_2$ start up limiting the concentration of activated chlorine ClO_x.

$$ClO + NO_2 + M \rightarrow ClONO_2 + M \tag{R8}$$

As we discussed previously, R7 will take place under sunlight conditions. Further, the following reactions will become relevant (Crutzen et al., 1992).

$$ClO + NO \rightarrow Cl + NO_2 \tag{R9}$$

$$Cl + CH_4 \rightarrow HCl + CH_3 \tag{R10}$$

$$HOCl + HCl \rightarrow Cl_2 + H_2O \tag{R11}$$

Reaction R11 takes place rapidly on pure or nitric acid doped ice-surfaces (Hanson and Ravishankara, 1992) and on NAT particles it was reported in Abbatt and Molina (1992).

2.1.2 Importance of gas phase reaction in stratospheric conditions

Since HOCl is supposed to be produced from the gas phase reactions, HO_2 is considered to be most important specie that helps in producing HOCl (Crutzen et al., 1992).

$$O_3 + h\nu(\lambda \leq 310nm) \rightarrow O(^1D) + O_2 \tag{R12}$$
$$O(^1D) + H_2O \rightarrow 2OH \tag{R13}$$
$$OH + O_3 \rightarrow HO_2 + O_2 \tag{R14}$$
$$CH_2O + h\nu(+2O_2) \rightarrow CO + 2HO_2 \tag{R15}$$
$$ClO + HO_2 \rightarrow HOCl + O_2 \tag{R16}$$

For the heterogeneous reaction to proceed, gas phase reactions play an important role as HO_2 is generating HOCl from R15 (Crutzen et al., 1992). In case of enough ClO in stratosphere, HO_2 will react to produce HOCl. And this condition is achieved only in polar night conditions followed up by R5, R6 and R4 (Crutzen et al., 1992). Under these conditions, any HO_x radical produced will breakdown a HCl molecule to form

activated chlorine molecule ClO_x (Crutzen et al., 1992), which is described as follows;

$$\begin{aligned} ClO + HO_2 &\rightarrow HOCl + O_2 && \text{(R16)} \\ HOCl + HCl &\rightarrow Cl_2 + H_2O && \text{(R11)} \\ Cl_2 + h\nu &\rightarrow 2Cl && \text{(R7)} \\ Cl + O_3 &\rightarrow ClO + O_2 \quad (2\times) && \text{(R4)} \\ \text{Net CR2}: \quad HCl + HO_2 + 2O_3 &\rightarrow ClO + H_2O + 3O_2 && \text{(R17)} \end{aligned}$$

The reaction cycle CR2, shows the importance of gas phase reactions to activate chlorine and to convert HCl to ClO_x. As the HCl reservoir species is reproduced under sunlight conditions via reaction R10, it is essential that HO_x is produced at a rapid rate resulting in the production of HOCl. Here the reaction

$$ClO + CH_3O_2 \rightarrow ClOO + CH_3O \qquad \text{(R18)}$$

turns out to be essential (Crutzen et al., 1992). In particular, the following cycle will be essential; this cycle continues and keeps activating and deactivating chlorine (Crutzen et al., 1992);

$$\begin{aligned} Cl + CH_4 &\rightarrow HCl + CH_3 && \text{(R10)} \\ ClO + CH_3O_2 &\rightarrow ClOO + CH_3O && \text{(R18)} \\ CH_3O + O_2 &\rightarrow CH_2O + HO_2 && \text{(R19)} \\ ClO + HO_2 &\rightarrow HOCl + O_2 && \text{(R16)} \\ HOCl + HCl &\rightarrow Cl_2 + H_2O && \text{(R11)} \\ Cl_2 + h\nu &\rightarrow 2 \quad Cl && \text{(R7)} \\ Cl + O_3 &\rightarrow ClO + O_2 \quad (2\times) && \text{(R4)} \\ \text{Net Reaction}: \quad CH_4 + 2O_3 &\rightarrow CH_2O + H_2O + 2O_2 && \text{(R20)} \end{aligned}$$

The net cycle reaction, shows that the methane oxidation is implying the formation of formaldehyde (CH_2O). The photolysis of formaldehyde will be considered in the next section because one sensitivity study is based on the breakdown of formaldehyde by photolysis.

2.2 Halogen chemistry in stratosphere

The inorganic chlorine and bromine compounds are important because their total abundance increases; they have different reaction rates, stability and transport phenomena from troposphere to stratosphere. Mostly, for sunlight conditions, inorganic bromine atom is more reactive and can be found as BrO.
The heterogeneous reaction of HCl and $ClONO_2$ on sulphate aerosol or on liquid and solid PSC surfaces forming Cl_2 can change the reservoirs to active species, and it is known as the central chlorine activation process (von Hobe and Stroh, 2012). HOCl production is based on HO_x and thus the more rapid the production of HOCl, the more rapidly HCl will be activated. The activated Cl with then deplete ozone. HOBr can react with HCl heterogeneously to produce BrCl, which enhances the active chlorine (ClO_x) concentrations (von Hobe and Stroh, 2012). Halogen molecules are important for ozone depletion in the global stratosphere; in particular in the upper stratosphere:

$$O_3 + h\nu \rightarrow O_2 + O \quad \text{(R21)}$$

$$XO + O \rightarrow X + O_2 \quad \text{(R22)}$$

$$X + O_3 \rightarrow XO + O_2 \quad \text{(R23)}$$

$$\text{Net X1}: \quad 2\ O_3 \rightarrow 3\ O_2 \quad \text{(R24)}$$

X stands for a halogen atom (mainly X equals to chlorine or bromine), and the reactions involved in ozone destruction, these halogen reactions are carried out by chlorine and bromine atoms. The above reaction cycle takes place with atomic oxygen, atomic oxygen in the atmosphere exists due to the UV radiation which dissociates ozone or oxygen molecules. The concentration of atomic oxygen depends on the intensity and photon energy of UV radiation along with the altitude (von Hobe and Stroh, 2012). Another cycle which is important in ozone destruction is carried out with the HO_2 radical, which can produce HOBr or HOCl. Therefore, following reactions would occur;

$$O_3 + OH \rightarrow HO_2 + O_2 \quad \text{(R25)}$$

$$XO + HO_2 \rightarrow HOX + O_2 \quad \text{(R26)}$$

$$HOX + h\nu \rightarrow X + OH \quad \text{(R27)}$$

$$X + O_3 \rightarrow XO + O_2 \quad \text{(R23)}$$

$$\text{Net X2}: \quad 2\ O_3 \rightarrow 3\ O_2 \quad \text{(R28)}$$

Production of halogen atom upon photolysis of the reservoir gases chlorine nitrate $ClONO_2$ and bromine nitrate $BrONO_2$ can produce activated halogen atoms which can dissociate ozone molecule (Toumi et al., 1993; Lary et al., 1996). $BrONO_2$ can heterogeneously hydrolyse to give HOBr (von Hobe and Stroh, 2012), but in this study we do not focus on the heterogeneous reaction with HOBr. HOBr can be photolyzed directly or can react heterogeneously with HCl to form BrCl which can be photolyzed (Lary et al., 1996). Heterogeneous ozone destruction cycles work in the presence of aerosol surface area and have the potential to generate HO_x from H_2O and ClO_x from HCl. As a general background of the halogen compounds reacting in upper stratosphere this part is being discussed in addition to the focus of this study.

$$NO + O_3 \rightarrow NO_2 + O_2 \quad \text{(R29)}$$
$$XO + NO_2 + M \rightarrow XONO_2 + M \quad \text{(R30)}$$
$$XONO_2 + h\nu \rightarrow X + NO_3 \quad \text{(R31)}$$
$$NO_3 + h\nu \rightarrow NO + O_2 \quad \text{(R32)}$$
$$X + O_3 \rightarrow XO + O_2 \quad \text{(R23)}$$
$$\text{Net X3}: \quad 2 \quad O_3 \rightarrow 3 \quad O_2 \quad \text{(R33)}$$

ClO_x and NO_x yet react in another gas-phase catalytic cycle;

$$O_3 + h\nu \rightarrow O_2 + O \quad \text{(R21)}$$
$$O + NO_2 \rightarrow NO + O_2 \quad \text{(R34)}$$
$$NO + ClO \rightarrow NO_2 + Cl \quad \text{(R35)}$$
$$Cl + O_3 \rightarrow ClO + O_2 \quad \text{(R4)}$$
$$\text{Net X4}: \quad 2 \quad O_3 \rightarrow 3 \quad O_2 \quad \text{(R36)}$$

2.2.1 The Dimer cycle

Molina and Molina (1987), figured out a cycle driven by ClO produced from heterogeneous activation. In this cycle ClO reacts with ozone without any atomic oxygen as shown in figure 2.1. The following reactions that presented by Molina and Molina

(1987) are:

$$\begin{aligned}
\mathrm{ClO} + \mathrm{ClO} + \mathrm{M} &\leftrightarrow \mathrm{ClOOCl} + \mathrm{M} && \text{(R1)}\\
\mathrm{ClOOCl} + \mathrm{h}\nu &\rightarrow \mathrm{Cl} + \mathrm{ClOO} && \text{(R2)}\\
\mathrm{ClOO} + \mathrm{M} &\rightarrow \mathrm{Cl} + \mathrm{O_2} + \mathrm{M} && \text{(R3)}\\
\mathrm{Cl} + \mathrm{O_3} &\rightarrow \mathrm{ClO} + \mathrm{O_2} \quad (2\times) && \text{(R4)}\\
\text{Net X5}: \quad 2 \quad \mathrm{O_3} &\rightarrow 3 \quad \mathrm{O_2} && \text{(R37)}
\end{aligned}$$

The ClO dimer cycle is initiated by the reaction of two ClO radicals as in R1, and this reaction takes place at high ClO concentrations, cold temperatures and high pressures. The ClOOCl formation has been confirmed by determining its rate constant in many laboratory experiments from flash photolysis with time resolved UV absorption spectroscopy (Nickolaisen et al., 1994). And same is true for the thermal dissociation of ClOOCl back into ClO (von Hobe and Stroh, 2012). Both these rate constants for ClOOCl and ClO formation have a significant effect on partitioning of active chlorine. Figure 2.1 represents the Dimer cycle, the chemical compound ClOOCl or Cl_2O_2 which is the Dimer, dissociates in the presence of sunlight resulting in generating active chlorine atoms. ClOO also dissociates into the active Cl atom and oxygen molecule. The two active chlorine atoms react instantly with an ozone molecule to dissociate the ozone molecule into one inert oxygen molecule O_2 and a ClO molecule.

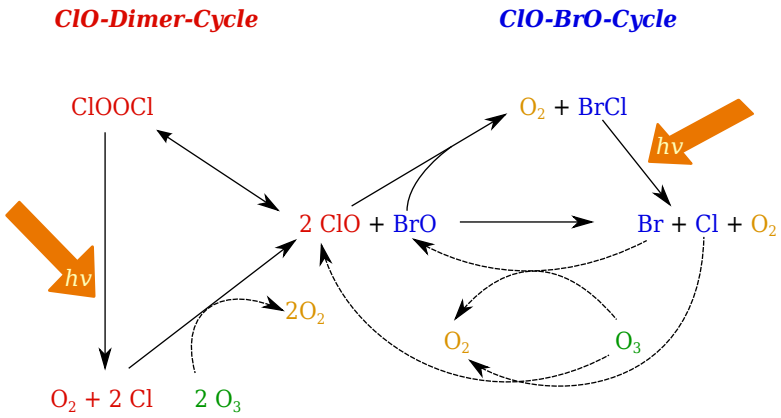

Figure 2.1: ClO-ClO and ClO-BrO Cycle (figure adapted from von Hobe and Stroh, 2012).

2.2.2 ClO-BrO cycle

In the ClO/BrO cycle as shown in figure 2.1, ClO and BrO combine to form Cl and Br atoms, which react with ozone molecules. This constitutes an important ozone depletion process (McElroy et al., 1986). BrCl, OClO and Br form respectively as shown in the reactions below. The first two reactions shown in the chain of the ClO/BrO cycle result in catalytic ozone removal. On the other hand, OClO is photolyzed to give an oxygen atom which reacts with an O_2 molecule to produce an O_3 molecule. Therefore, branching of these first three reactions into different channels is the key parameter to determine ozone loss by this catalytic cycle (von Hobe and Stroh, 2012). Laboratory studies on the branching ratios and individual reaction rate constants as a function of stratospheric temperatures are in good agreement with field observations. Kawa et al. (2009) identified the $ClO + BrO$ reaction and its branching ratios confiding uncertainties in modelling polar ozone depletion and projecting future changes in response to changing halogen emissions and climate. The reaction cycle $ClO + BrO$ proceeds faster when there is more ClO present, which underlines the importance of chlorine activation. Partitioning of activated chlorine ClO_x into ClO and its dimer is also important because not all ClO will participate in the ClO/BrO cycle. The ozone loss rate depends upon the ClO dimer photolysis rate more than on any other parameter in reaction kinetics.

$$
\begin{aligned}
ClO + BrO &\rightarrow Cl + Br + O_2 && \text{(R38)}\\
&\rightarrow BrCl + O_2 && \text{(R39)}\\
&\rightarrow OClO + Br && \text{(R40)}\\
BrCl + h\nu &\rightarrow Br + Cl && \text{(R41)}\\
Cl + O_3 &\rightarrow ClO + O_2 && \text{(R4)}\\
Br + O_3 &\rightarrow BrO + O_2 && \text{(R42)}\\
\text{Net X6}: \quad 2 \quad O_3 &\rightarrow 3 \quad O_2 && \text{(R43)}
\end{aligned}
$$

2.2.3 ClO Dimer Photolysis

Before beginning the explanation of dimer photolysis, it is essential to present some basics of photolysis. In the atmosphere, the photolysis rate is described by the product of actinic flux, absorption cross section and quantum yield, all of these fields are integrated

over the specific wavelength to obtain the photolysis rate.

$$J = \int_{\lambda} I(\lambda) \cdot \phi(\lambda) \cdot \sigma(\lambda)\, d(\lambda) \tag{2.1}$$

Where,
J = Photolysis rate (s^{-1}) .
$I(\lambda)$ = Actinic flux (*Quanta or photons*/m^2 nm S). $I(\lambda) \propto$ probability of photon near molecule.
$\sigma(\lambda)$ = Absorption cross section (cm^2/molecule). $\sigma(\lambda) \propto$ probability that photon is absorbed.
$\phi(\lambda)$ = Photo dissociation quantum yield (*molecule*/*quanta or photon*). $\phi(\lambda) \propto$ probability that the absorbed photon causes dissociation.
λ = Wavelength range (nm).

$$AB + h\nu \rightarrow A + B \tag{R44}$$

The rate of the above reaction R44 will be defined as;

$$\text{Reactants} = \frac{d[AB]}{dt}|_{h\nu} = -J[AB] \tag{2.2}$$

$$\text{Products} = \frac{d[A]}{dt}|_{h\nu} = \frac{d[B]}{dt}|_{h\nu} = +J[AB] \tag{2.3}$$

The actinic flux $I(\lambda)$ depends on a number of atmospheric parameters including solar zenith angle and altitude as well as the presence and quantity of other absorbing species and aerosol particles (von Hobe and Stroh, 2012). The photolysis cross section is given by the absorption cross section $\sigma(\lambda)$ multiplied by the photolysis quantum yield $\phi(\lambda)$, both of these quantities are determined in laboratory studies. For dimer photolysis (ClOOCl), many studies agreed upon the photolysis quantum yield equals to unity for specific wavelength (Plenge et al., 2004). However, there are significant differences in the published ClOOCl absorption cross section or UV-visible absorption spectra (Pope et al., 2007; von Hobe et al., 2009). Earlier studies carried out in 1980s and 1990s were focused on ClO_x partitioning and ozone loss (Santee et al., 2008; Stimpfle et al., 2004; von Hobe et al., 2007). Pope et al. (2007) published a ClOOCl absorption spectrum which resulted in very low Cl_2O_2 photolysis rates with the implication of a very slow ClO dimer cycle that would not allow the observed ozone loss in Antarctic and Arctic winters to be simulated. However, that study revealed the method to measure ClOOCl

absorption cross section quite accurately because a method to prepare pure ClOOCl was developed by Pope et al. (2007). After the method discovered by Pope et al. (2007), a Cl_2 impurity was found in the procedure which was testified later by von Hobe et al. (2009). Based on many experimental studies absolute ClOOCl cross sections are poorly established. Extremely low values suggested by Pope et al. (2007) would rise the question to understand the catalytic behaviour of chemical reactions leading to polar ozone depletion. More recently however, a laboratory study on the Cl_2O_2 dimer photolysis, confirms a substantial role of the Cl_2O_2 dimer on Antarctic ozone loss (Papanastasiou et al., 2009).

3 Model description

The simulations presented in this study were performed with CLaMS (McKenna et al., 2002b,a; Konopka et al., 2004; Grooß et al., 2005). The simulations is based on the study performed by Grooß et al. (2011). A single air parcel trajectory is assumed from Antarctic winter to Antarctic spring, where the ozone hole appears every year (section 1.5, see also WMO, 2014). In this box-model mode, a single air parcel is described by the location of the lowest ozone value during the ozone hole period (Grooß et al., 2011), and two trajectories are introduced in the box-model environment, where the first trajectory runs backward towards the month of June while the second runs forward towards the month of December. Model simulations run with the combination of these two trajectories forward using the CLaMS chemistry module (Grooß et al., 2011). Wind and temperature data for the single air parcel trajectory are taken from the ERA-Interim reanalysis (Dee et al., 2011) with the resolution of $1^\circ \times 1^\circ$. Diabatic descent rates were determined from a radiation code (Morcrette, 1991; Zhong and Haigh, 1995), and these diabatic descent rates are used assuming cloud free atmosphere based on temperatures from the ERA-Interim reanalysis (Dee et al., 2011) and climatological ozone and water vapour profiles (Grooß and Russell, 2005; Grooß et al., 2011). CLaMS uses different integration methods to solve stiff ordinary differential equations describing the chemistry (Carver et al., 1997; McKenna et al., 2002a). The chemical kinetics of the trajectory are based upon Sander et al. (2011b). The photolysis rates are calculated for spherical geometry (Meier et al., 1982; Becker et al., 2000) on hourly basis using climatological ozone profile and ozone hole conditions from HALOE measurements (Grooß and Russell, 2005; Grooß et al., 2011).

Heterogeneous chemistry is calculated on ice, nitric acid trihydrate (NAT), liquid ternary particles ($H_2O/H_2SO_4/HNO_3$) and cold liquid binary aerosols (Grooß et al., 2011). Temperature dependent uptake coefficients of heterogeneous reactions on liquid ternary and binary aerosols are parametrised by Shi et al. (2001). The parametrisations of uptake coefficients for reaction on NAT is used from Carslaw and Peter (1997), based on the laboratory measurements of Hanson and Ravishankara (1993). NAT particles are

assumed to form from super ternary solutions (STS) droplets upon cooling, HNO_3 supersaturates with respect to NAT, when it reached below 10 folds lower to the threshold of T_{NAT} that is $\sim$ 3K super-cooling (McKenna et al., 2002a; Grooß et al., 2011). The NAT number density is set to 0.003 cm^{-3} in contrast to Grooß et al. (2011).
In the box-model mode, SVODE (Brown et al., 1989) solver is utilised. SVODE is essential in particular for stiff systems, which is helpful for different time steps and reaction rate orders. For several reactions with different reaction rates, SVODE is applied to not proceed the next time step until the previous time step completes, which gives higher accuracy in the interpolated results. SVODE adapts the integration step such that a pre-defined accuracy is satisfied. SVODE does not use simplifications like the family concept that is used in IMPACT solver.
In the model, denitrification is neglected, the effect of denitrification is analysed by sensitivity studies. The results from box-model does not take into account mixing between neighbouring air masses and neither the air parcel involved in denitrification due to sedimentation of HNO_3 contain particles (Grooß et al., 2011). The box-model environment is modified to analyse the chemical processes in the region of low ozone mixing ratios to interpret the chemistry of stratosphere involved during the lowest ozone mixing ratios.
The CLaMS model version contains broad series of reactions presented in different studies that are taking place in stratosphere, CLaMS includes full chlorine and bromine chemistry, 37 chemical species, and 130 reactions involving photolysis and heterogeneous reactions. The model chemistry is integrated based upon Atmospheric Chemistry Code (ASAD) presented by Carver et al. (1997), which provides a subroutine to solve atmospheric chemistry time dependent problems, a chemical reaction database and utility programs. ASAD subroutine provides a choice of published integrator solver methods to deal with atmospheric chemistry modelling; here the SVODE solver (Brown et al., 1989) is used.
The chemical reactions (see table 3.1) consist of gas-phase, trimolecular or thermal decomposition, photolysis and heterogeneous reactions. The rate coefficients are calculated by the temperature and pressure dependent routines followed by Sander et al. (2011b), included in CLaMS model. The photolysis rate [s^{-1}] mainly depends upon solar zenith angle, atmospheric ozone profile, and surface albedo. In CLaMS, reaction rates are determined at every hour, and the time interval is variable.

Table 3.1: Gas-phase (B1-B64) presented in McKenna et al. (2002a) and updated gas-phase reactions from (B65-B83) presented by Grooß et al. (2014) are included in this table, tri-molecular reactions (T13) is added from the study of Grooß et al. (2014), Photolysis (J28-J36) are included in the model followed by Grooß et al. (2014), and Heterogeneous reactions included in CLaMS chemistry module presented by McKenna et al. (2002a)

	Reaction
B1	$O(^3P) + O_3 \rightarrow O_2 + O_2$
B2	$O(^1D) + O_2 \rightarrow O(^3P) + O_2$
B3	$O(^1D) + H_2O \rightarrow OH + OH$
B4	$O(^1D) + H_2 \rightarrow OH + H$[1]
B5	$O(^1D) + N_2 \rightarrow O(^3P) + N_2$
B6	$O(^1D) + CH_4 \rightarrow OH + CH_3$
B7	$OH + O_3 \rightarrow HO_2 + O_2$
B8	$OH + HO_2 \rightarrow H_2O + O_2$
B9	$OH + H_2O_2 \rightarrow H_2O + HO_2$
B10	$HO_2 + O_3 \rightarrow OH + 2O_2$
B11	$HO_2 + HO_2 \rightarrow H_2O_2 + O_2$
B12	$O(^3P) + NO_2 \rightarrow NO + O_2$
B13	$OH + NO_3 \rightarrow HO_2 + NO_2$
B14	$OH + HNO_3 \rightarrow H_2O + NO_3$
B15	$OH + HO_2NO_2 \rightarrow NO_2 + H_2O + O_2$
B16	$HO_2 + NO \rightarrow NO_2 + OH$
B17	$HO_2 + NO_3 \rightarrow NO_2 + OH + O_2$
B18	$NO + O_3 \rightarrow NO_2 + O_2$
B19	$NO + NO_3 \rightarrow NO_2 + NO_2$
B20	$NO_2 + O_3 \rightarrow NO_3 + O_2$
B21	$OH + CO \rightarrow CO_2 + H$
B22	$OH + CH_4 \rightarrow H_2O + CH_3$
B23	$OH + CH_2O \rightarrow H_2O + HCO$
B24	$OH + CH_3OH \rightarrow H_2O + CH_2O + H$
B25	$OH + CH_3OOH \rightarrow CH_3OO + H_2O$
B26	$OH + CH_3OOH \rightarrow CH_2O + OH + H_2O$
B27	$HO_2 + CH_3OO \rightarrow CH_3OOH + O_2$

[1]Model realization of the species $HCO, H, ClOO$, and CH_3 which are assumed to react instantaneously to $CO + HO_2, HO_2, Cl + O_2$, and CH_3O_2, respectively.

Table 3.1 continued

	Reaction
B28	$CH_3OO + CH_3OO \rightarrow CH_3OH + CH_2O + O_2$
B29	$CH_3OO + NO \rightarrow NO_2 + CH_2O + H$
B30	$CH_3OOH + Cl \rightarrow HCl + CH_2O + OH$
B31	$O(^3P) + ClO \rightarrow Cl + O_2$
B32	$OH + Cl_2 \rightarrow HOCl + Cl$
B33	$OH + ClO \rightarrow HO_2 + Cl$
B34	$OH + ClO \rightarrow HCl + O_2$
B35	$OH + HCl \rightarrow H_2O + Cl$
B36	$OH + HOCl \rightarrow H_2O + ClO$
B37	$HO_2 + Cl \rightarrow HCl + O_2$
B38	$HO_2 + Cl \rightarrow OH + ClO$
B39	$HO_2 + ClO \rightarrow HOCl + O_2$
B40	$Cl + O_3 \rightarrow ClO + O_2$
B41	$Cl + H_2 \rightarrow HCl + H$
B42	$Cl + CH_4 \rightarrow HCl + CH_3$
B43	$Cl + CH_2O \rightarrow HCl + HCO$
B44	$Cl + CH_3OH \rightarrow HCl + CH_2O + H$
B45	$Cl + OClO \rightarrow ClO + ClO$
B46	$Cl + HOCl \rightarrow Cl_2 + OH$
B47	$Cl + HOCl \rightarrow ClO + HCl$
B48	$Cl + ClONO_2 \rightarrow Cl_2 + NO_3$
B49	$ClO + NO \rightarrow NO_2 + Cl$
B50	$ClO + CH_3OO \rightarrow Cl + CH_2O + HO_2$
B51	$O(^3P) + BrO \rightarrow Br + O_2$
B52	$OH + HBr \rightarrow H_2O + Br$
B53	$HO_2 + Br \rightarrow HBr + O_2$
B54	$HO_2 + BrO \rightarrow HOBr + O_2$
B55	$Br + O_3 \rightarrow BrO + O_2$
B56	$Br + CH_2O \rightarrow HBr + HCO$
B57	$BrO + NO \rightarrow NO_2 + Br$
B58	$BrO + ClO \rightarrow Br + OClO$
B59	$BrO + ClO \rightarrow Br + Cl + O_2$
B60	$BrO + ClO \rightarrow BrCl + O_2$

Table 3.1 continued

	Reaction
B61	$BrO + BrO \rightarrow Br + Br + O_2$
B62	$BrO + BrO \rightarrow Br_2 + O_2$
B63	$O(^3P) + HOBr \rightarrow OH + BrO$
B64	$OH + Br_2 \rightarrow HOBr + Br$
B65	$H + O_3 \rightarrow OH + O_2$
B66	$H + HO_2 \rightarrow OH + OH$
B67	$H + HO_2 \rightarrow H_2O + O(^3P)$
B68	$H + HO_2 \rightarrow H_2 + O_2$
B69	$H_2 + OH \rightarrow H_2O + H$
B70	$OH + O(^3P) \rightarrow H + O_2$
B71	$OH + OH \rightarrow H_2O + O(^3P)$
B72	$HO_2 + O(^3P) \rightarrow OH + O_2$
B73	$H_2O_2 + O(^3P) \rightarrow OH + HO_2$
B74	$O(^3P) + HOCl \rightarrow OH + ClO$
B75	$N_2O + O(^1D) \rightarrow N_2 + O_2$
B76	$N_2O + O(^1D) \rightarrow NO + NO$
B77	$CCl_3F + O(^1D) \rightarrow ClO + 2Cl + \text{products}$
B78	$CCl_2F_2 + O(^1D) \rightarrow ClO + Cl + \text{products}$
B79	$CHClF_2 + O(^1D) \rightarrow ClO + H + \text{products}$
B80	$CCl_3F_3 + O(^1D) \rightarrow ClO + 2Cl + \text{products}$
B81	$CCl_4 + O(^1D) \rightarrow 3Cl + ClO + \text{products}$
B82	$CHClF_2 + OH \rightarrow Cl + H_2O + \text{products}$
B83	$CH_3Cl + OH(+O_2) \rightarrow ClO + CH_3OOH$
T1	$O(^3P) + O_2 + M \rightarrow O_3$
T2	$OH + NO_2 + M \rightarrow HNO_3$
T3	$HO_2 + NO_2 + M \rightarrow HO_2NO_2$
T4	$HO_2NO_2 + M \rightarrow HO_2 + NO_2$
T5	$NO_2 + NO_3 + M \rightarrow N_2O_5$
T6	$N_2O_5 + M \rightarrow NO_2 + NO_3$
T7	$CH_3OO + NO_2 + M \rightarrow CH_3O_2NO_2$
T8	$CH_3O_2NO_2 + M \rightarrow CH_3OO + NO_2$
T9	$ClO + NO_2 + M \rightarrow ClONO_2$
T10	$ClO + ClO + M \rightarrow Cl_2O_2$

Table 3.1 continued

	Reaction
T11	$Cl_2O_2 + M \rightarrow 2ClO$
T12	$BrO + NO_2 + M \rightarrow BrONO_2$
T13	$H + O_2 + M \rightarrow HO_2$
J1	$BrONO_2 + h\nu \rightarrow BrO + NO_2$
J2	$BrONO_2 + h\nu \rightarrow Br + NO_3$
J3	$BrCl + h\nu \rightarrow Br + Cl$
J4	$Cl_2 + h\nu \rightarrow 2Cl$
J5	$Cl_2O_2 + h\nu \rightarrow Cl + ClOO$
J6	$ClNO_2 + h\nu \rightarrow Cl + NO_2$
J7	$ClONO_2 + h\nu \rightarrow Cl + NO_3$
J8	$ClONO_2 + h\nu \rightarrow ClO + NO_2$
J9	$H_2O_2 + h\nu \rightarrow 2OH$
J10	$CH_2O + h\nu \rightarrow HCO + H$
J11	$CH_2O + h\nu \rightarrow H_2 + CO$
J12	$HO_2NO_2 + h\nu \rightarrow HO_2 + NO_2$
J13	$HO_2NO_2 + h\nu \rightarrow OH + NO_3$
J14	$HOBr + h\nu \rightarrow OH + Br$
J15	$HOCl + h\nu \rightarrow OH + Cl$
J16	$HNO_3 + h\nu \rightarrow OH + NO_2$
J17	$CH_3O_2NO_2 + h\nu \rightarrow CH_3OO + NO_2$
J18	$CH_3OOH + h\nu \rightarrow CH_2O + OH + H$
J19	$N_2O_5 + h\nu \rightarrow NO_3 + NO_2$
J20	$NO_2 + h\nu \rightarrow NO + O(^3P)$
J21	$NO_3 + h\nu \rightarrow NO_2 + O(^3P)$
J22	$NO_3 + h\nu \rightarrow NO_2 + O(^3P)$
J23	$O_2 + h\nu \rightarrow O(^3P) + O(^3P)$
J24	$O_3 + h\nu \rightarrow O_2 + O(^3P)$
J25	$O_3 + h\nu \rightarrow O_2 + O(^1D)$
J26	$OClO + h\nu \rightarrow O(^3P) + ClO$
J27	$Br_2 + h\nu \rightarrow Br + Br$
J28	$HCl + h\nu \rightarrow H + Cl$
J29	$H_2O + h\nu \rightarrow H + OH$
J30	$CCl_3F + h\nu \rightarrow 3Cl + \text{products}$

Table 3.1 continued

	Reaction
J31	$CCl_2F_2 + h\nu \rightarrow 2Cl + \text{products}$
J32	$CHClF_2 + h\nu \rightarrow Cl + H + \text{products}$
J33	$CCl_3F_3 + h\nu \rightarrow 3Cl + \text{products}$
J34	$CH_3Cl + h\nu(+O_2) \rightarrow CH_3OO + Cl$
J35	$CCl_4 + h\nu \rightarrow 4Cl + \text{products}$
J36	$N_2O + h\nu \rightarrow O(^1D) + N_2$
H1	$ClONO_2 + H_2O \rightarrow HOCl + HNO_3$
H2	$ClONO_2 + HCl \rightarrow Cl_2 + HNO_3$
H3	$HOCl + HCl \rightarrow Cl_2 + H_2O$
H4	$N_2O_5 + H_2O \rightarrow HNO_3 + HNO_3$
H5	$N_2O_5 + HCl \rightarrow ClNO_2 + HNO_3$
H6	$ClONO_2 + HBr \rightarrow BrCl + HNO_3$
H7	$BrONO_2 + HCl \rightarrow BrCl + HNO_3$
H8	$HOCl + HBr \rightarrow BrCl + H_2O$
H9	$HOBr + HCl \rightarrow BrCl + H_2O$
H10	$HOBr + HBr \rightarrow Br_2 + H_2O$
H11	$BrONO_2 + H_2O \rightarrow HOBr + HNO_3$

4 Results and Discussion

4.1 Standard Run

The trajectory which is selected to analyse the stratospheric chemistry in the vortex core during late winter and early spring, covers the period when lowest ozone mixing ratios are observed. The selected trajectory intersects an observation of South Pole Station of about 10 ppbv ozone at the pressure level of 70 hPa on 24^{th} of September, 2003. This trajectory was used already in the study by Grooß et al. (2011). The simulated time duration for all the runs performed by CLaMS is from 1^{st} of June to 30^{th} of November, 2003. The trajectory stays in the vortex core around 77°S with a standard deviation of 5°. A representation of the trajectory is presented in the figure 4.1, describing the chemistry in stratosphere during late winter in Antarctica and the behaviour of chemical reactions till early spring. The diabatic descent is shown in figure 4.1 (panel a), the air parcel descends to an altitude where lowest ozone values are observed, that is around 390 K. This air parcel is presumed to move in the same path along the vortex core, since no mixing is assumed. Panels b and c show temperature and solar zenith profile along the trajectory. It is known that low temperatures are the reason for heterogeneous chlorine activation and ozone depletion (Solomon, 1999; Drdla and Müller, 2012). In figure 4.1 panel b, the dotted line at temperature 195 K represents the temperature threshold T_{NAT}, at which Nitric acid trihydrate (NAT) can exist but is unlikely to form, but supercooling of about 3K below T_{NAT} is necessary to propagate NAT formation (Peter and Grooß, 2012). Throughout winter and early spring the temperature is about below the T_{NAT} threshold. Further, independently of the formation of NAT particles, T_{NAT} is the temperature below which heterogeneous chemistry sets on (Drdla and Müller, 2012), which drives the heterogeneous chemistry to accelerate the reactions to activate chlorine. The initial titration between HCl and $ClONO_2$ occurred before June, which activated chlorine in the form of ClO_x. Thus ClO_x starts from 1 ppb in the model simulation with a near zero value of $ClONO_2$. There is no significant effect of ClO_x on ozone during polar night when there is a large solar zenith angle as shown in panel c. In

early spring, solar zenith angle is much lower. Under sunlight conditions, the Cl_2 resulting from heterogeneous reactions is photolyzed to form ClO_x and the HCl mixing ratio shows the opposite behaviour to chlorine activation. HCl is consumed heterogeneously to further activate chlorine during early spring. Low temperatures allow heterogeneous reactions to proceed rapidly. The main heterogeneous reaction that activates chlorine is $HOCl + HCl$, which produces Cl_2 that photolyzes to form ClO_x. HOCl is formed in the gas-phase reaction (Prather, 1992; Crutzen et al., 1992).

$$ClO + HO_2 \rightarrow HOCl + O_2 \tag{R16}$$

The HOCl formed in reaction R16 is then reacting heterogeneously (Prather, 1992; Crutzen et al., 1992);

$$HOCl + HCl \rightarrow Cl_2 + H_2O \tag{R11}$$

The importance of the heterogeneous reaction, of $ClONO_2$ with HCl was presented by Solomon et al. (1986). This reaction describes chlorine activation as given in reaction R6.

$$ClONO_2 + HCl \rightarrow Cl_2 + HNO_3 \tag{R6}$$

In figure 4.2 panel a, the rates of reaction R11 and R6 are shown and similarly in panel b, the rates for reaction R16 and R8 are presented respectively.

$$ClO + HO_2 \rightarrow HOCl + O_2 \tag{R16}$$

$$ClO + NO_2 + M \rightarrow ClONO_2 + M \tag{R8}$$

In figure 4.2 we compare the relative importance of the heterogeneous reactions R16 and R8. In panel a, the rate of reaction R11 shown in red is dominant throughout the duration of simulation till the month of October. Especially, when the lowest ozone mixing ratios are observed in late September, the rate of reaction R11 is substantially more rapid than the rate of reaction R6. Similarly panel b represents the reaction rates in which HOCl and $ClONO_2$ are produced and their temporal development shows the resemblance with the panel a in figure 4.2.

As long as high concentrations of ClO dominate the chlorine partitioning; the HO_2 required to initiate reaction R16, is produced from the photolysis of CH_2O (radical

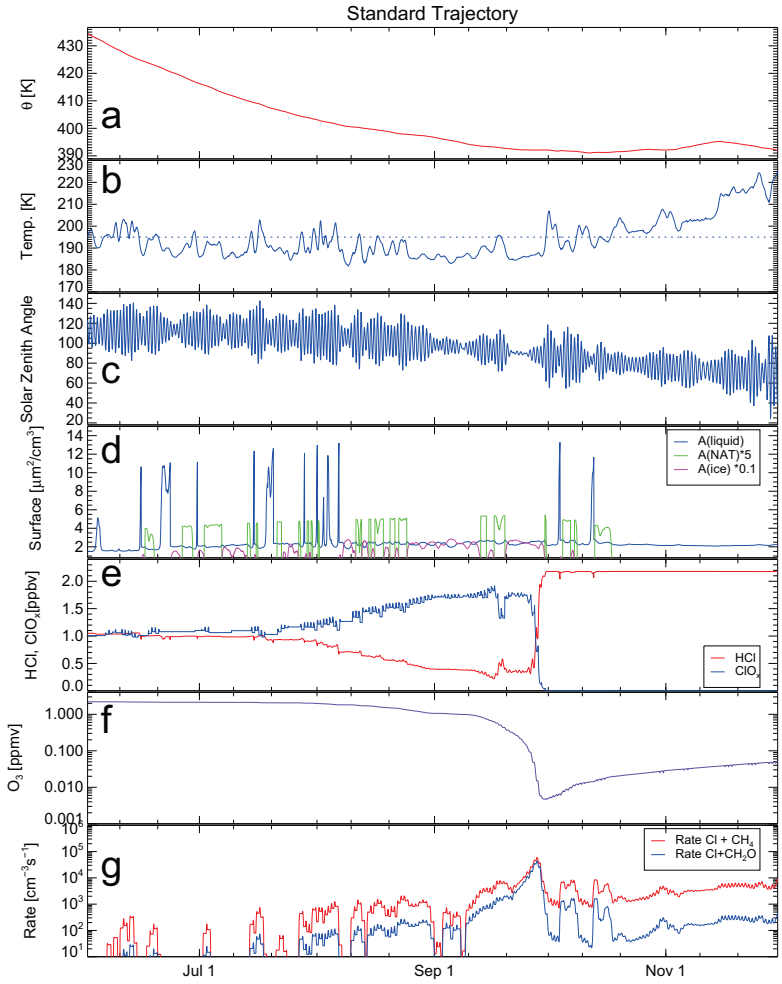

Figure 4.1: Box-model simulation of a trajectory, which intersects the observation of ozone sonde for 10 ppbv of ozone mixing ratio at 73 hPa on 24 September 2003. Time series of Box-model simulation is presented in different panels with different parameters such as: (a) Potential temperature of air parcel, (b) assimilated temperature from the ECMWF dataset, (c) Solar Zenith Angle, (d) HCl (red) and ClO_x (blue), (e) Surface area density of Nitric acid trihydrate (NAT) in green scaled by a factor 5, liquid aerosol in blue and ice in orchid scaled by a factor of 0.1, (f) Ozone mixing ratio (Violet) and (g) Reaction rates of atomic chlorine with CH_4 (red) and CH_2O (blue), and the rates are averaged by 24 hour for clear plotting.

channel reaction R47 which produces HO_2).

$$CH_2O + h\nu \rightarrow H_2 + CO \tag{R46}$$

$$CH_2O + h\nu \rightarrow HCO + H \tag{R47}$$

Under these conditions, the formation of $ClONO_2$ in reaction R8 is inhibited due to the lack of available NO_2.

$$ClO + NO_2 + M \rightarrow ClONO_2 + M \tag{R8}$$

In the presence of PSCs at low temperatures, formation of HOCl starts from the reaction R16 where the produced HOCl is immediately consumed by heterogeneous reaction with HCl from the reaction R11. And this phase is a chlorine activation phase, because R11 produces Cl_2, which upon photolysis is converted into atomic chlorine Cl. Atomic chlorine reacts with O_3 to ClO and the ClO dimer cycle takes place to deplete ozone. In figure 4.1 panel d, HCl is declining initially and ClO_x increases due to chlorine activation process.
During sunlight conditions in Antarctic spring, and with decreasing mixing ratios of O_3, the Cl/ClO ratio increases (Douglass et al., 1995; Grooß et al., 1997; Grooß et al., 2011) so that increasingly rapid HCl production via R10 and R45 takes place as shown in figure 4.1 panel d.

$$CH_4 + Cl \rightarrow HCl + CH_3 \tag{R10}$$

$$CH_2O + Cl \rightarrow HCl + CHO \tag{R45}$$

Since reaction R10 and R45 lead to chlorine deactivation, two reaction cycles are important which are presented below (Cycles C1 and C2). The importance of these two cycles means that the HCl production through reaction R10 and R45 restrains a net effect of zero. HCl produced by these two reactions is consumed heterogeneously by reaction R11. The net effect of HCl in these two null cycles can be demonstrated from the figure 4.1. Panel e illustrates the chlorine activation in terms of HCl. The low values of HCl in red, represents the activation and this activation is maximum in the last week of the September. In comparison with the panel g, where rates of the reaction are presented in red and blue for reaction R10 and R45 respectively, which produces HCl.

HCl is consumed heterogeneously in reaction R11, and activates chlorine in ClO_x. The chlorine activation mechanism is explained in the two cycles from the reaction R11, R7 and R4 resulting in the ozone depletion in panel f. Higher mixing ratios of activated chlorine ClO_x results in faster ozone depletion. In figure 4.3, panel a shows the mixing ratio of $ClONO_2$ with a log scale y-axis. $ClONO_2$ is produced in very low amounts, which confirms the weak NO_2 production during polar night. In figure 4.3, panel b represents the production of NO_x from the photolysis of HNO_3 and reaction of HNO_3 with OH. The two reaction cycles C1 and C2 are given by the reaction sequence:

$$\begin{aligned}
& CH_4 + Cl \rightarrow HCl + CH_3 && \text{(R10)}\\
& CH_3 + O_2 \rightarrow CH_3O_2 && \text{(R48)}\\
& CH_3O_2 + ClO \rightarrow CH_3O + Cl + O_2 && \text{(R18)}\\
& CH_3O + O_2 \rightarrow HO_2 + CH_2O && \text{(R19)}\\
& ClO + HO_2 \rightarrow HOCl + O_2 && \text{(R16)}\\
& HOCl + HCl \rightarrow Cl_2 + H_2O && \text{(R11)}\\
& Cl_2 \rightarrow 2Cl && \text{(R7)}\\
& Cl + O_3 \rightarrow ClO + O_2 \quad (2\times) && \text{(R4)}\\
\text{Net C1 :}\quad & CH_4 + 2O_3 \rightarrow CH_2O + H_2O + 2O_2
\end{aligned}$$

and by

$$\begin{aligned}
& CH_2O + Cl \rightarrow HCl + CHO && \text{(R45)}\\
& CHO + O_2 \rightarrow CO + HO_2 && \text{(R49)}\\
& ClO + HO_2 \rightarrow HOCl + O_2 && \text{(R16)}\\
& HOCl + HCl \rightarrow Cl_2 + H_2O && \text{(R11)}\\
& Cl_2 + h\nu \rightarrow 2\,Cl && \text{(R7)}\\
& Cl + O_3 \rightarrow ClO + O_2 \quad (2\times) && \text{(R4)}\\
\text{Net C2 :}\quad & CH_2O + 2\,O_3 \rightarrow CO + H_2O + 2O_2
\end{aligned}$$

It is shown that there is no net HCl production and these two reaction chains are null cycles for HCl production. It is evident that the reaction rate of R10 and R45 increases considerably the production of HCl mixing ratios in the month of September as shown in figure 4.1 panel g. However, these cycles cannot explain the decrease of HCl from the

values of ≈ 1 to 0.2 ppb in late August and September and complete chlorine activation of chlorine as observed (Santee et al., 2008).

Furthermore, when ozone reaches its lowest values, the HCl increases rapidly (Grooß

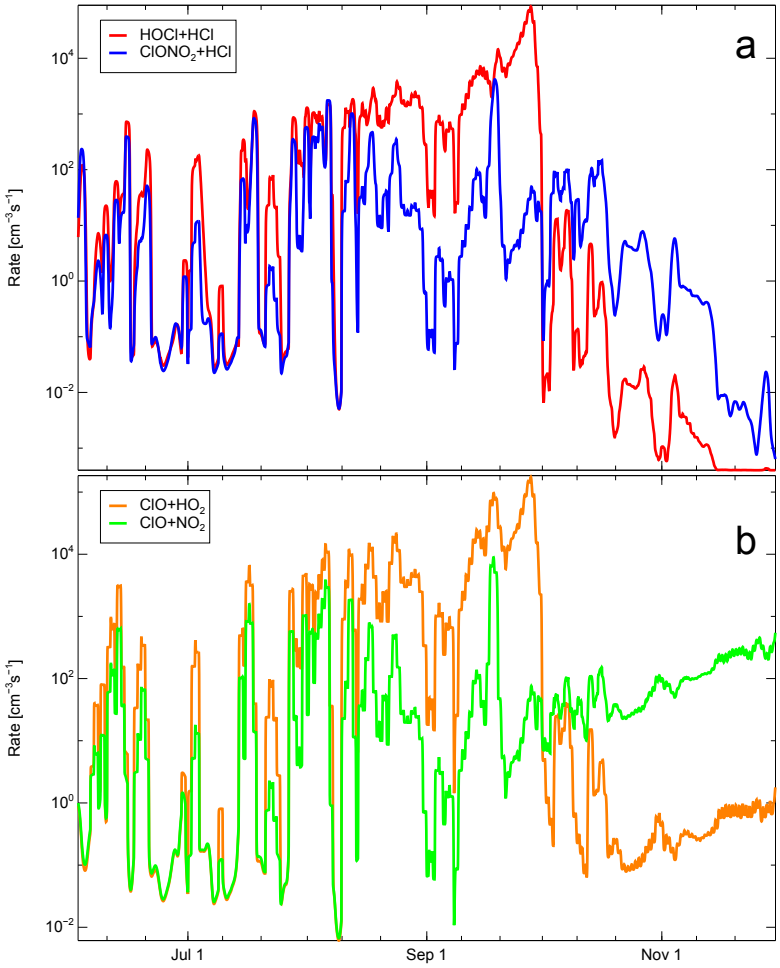

Figure 4.2: Reaction rates in $cm^{-3}s^{-1}$ for the reaction R11 and R6 in red and blue colour respectively, and in panel b, reaction R16 in orange and reaction R8 in green colour represents their respective rates.

et al., 2011), see also figure 4.1. The rapid increase of HCl and rapid decrease in ClO_x occurs at the same time. And chlorine deactivation into HCl happens and the concurrent decreases in ClO_x due to reaction R10 and R45. The simulated HCl begins to rise very rapidly, when extremely low ozone mixing ratios are observed (below 0.1 ppmv).

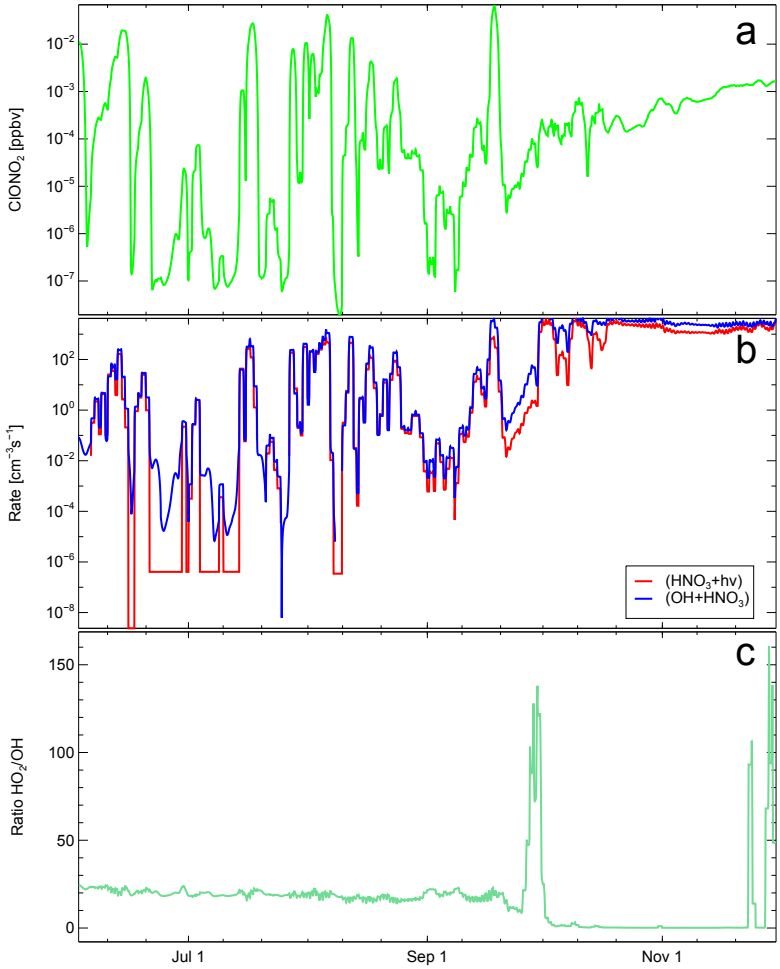

Figure 4.3: Production of $ClONO_2$ in panel a, panel b contains photolysis reaction rate of HNO_3 and $OH + HNO_3$ that proceed to the production of NO_x, panel c represents the ratio of HO_2 and OH.

4.2 The importance of the reaction $HOCl + HCl$ and $CH_3O_2 + ClO$ for "ozone hole" chemistry

Here we conduct a sensitivity study on the importance of the gas phase reaction R18 and the heterogeneous reaction R11 in ozone hole chemistry. The Crutzen et al. (1992) study identified the importance of gas phase reaction R18 which generates HO_x (HO_2) and subsequently forms HOCl to react heterogeneously on PSCs. In the Crutzen et al. (1992) study, the emphasis was on the heterogeneous reaction R11 and the heterogeneous reactions were assumed to take place on nitric acid trihydrate (NAT) particles. But in this box-model study, all the recommended heterogeneous reactions are permitted to take place on liquid particles, NAT and ice particles. Thus all the information obtained since 1992 on heterogeneous reactions is taken into account (Peter and Grooß, 2012). Same sensitivity studies are performed under the new and modified model. Plot resolution in the Crutzen et al. (1992) was modest. Simulation time steps were based on daily basis in the plots used by Crutzen et al. (1992). The ozone simulation of Crutzen et al. (1992) was unable to simulate the ozone reformation after the minimum O_3 was reached, which is improved in the latest box-model environment. The two reactions which represent importance of gas phase and heterogeneous phase are mentioned below.

$$HOCl + HCl \rightarrow Cl_2 + H_2O \tag{R11}$$

$$CH_3O_2 + ClO \rightarrow CH_3O + Cl + O_2 \tag{R18}$$

However, in this study, the cases are based on a study similar to Crutzen et al. (1992). Denitrification and dehydration is only accounted for in a simplified way in the new model. The gas-phase reaction R18 is considered to form formaldehyde, which speeds up the HO_x production through the photolysis of formaldehyde. Since CH_3O quickly reacts with O_2 to form formaldehyde and HO_2, R18 is realised in the model as follows:

$$\textit{In model}: \quad CH_3O_2 + ClO \rightarrow CH_2O + Cl + HO_2 \tag{R18}$$

Both the reactions R18 and R11 are involved in the methane oxidation cycle (Crutzen et al., 1992) resulting in formaldehyde formation. In the sensitivity study discussed below these two reactions are switched on and off alternatively which is described in the table below. Case A represents the standard run, hence no other assumptions are assumed specifically for the case A. All the simulations for ozone in this case study

	R11	R18
Case A	yes	yes
Case B	yes	no
Case C	no	yes
Case D	no	no

Table 4.1: Reactions in the sensitivity calculations

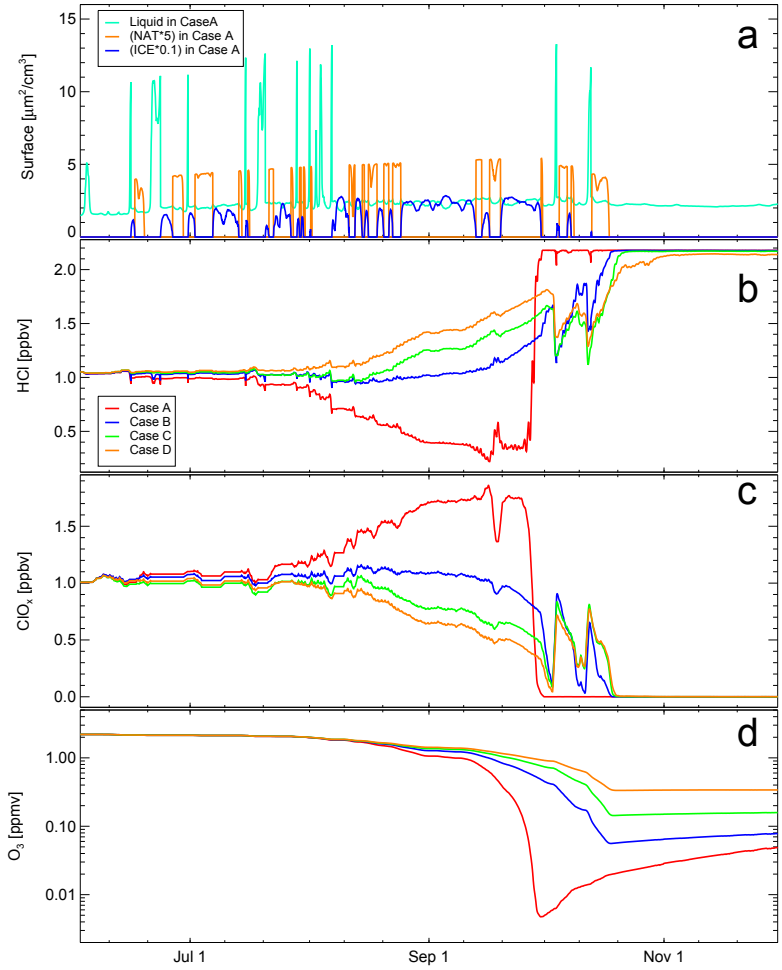

Figure 4.4: (a) Surface area density of NAT, ice and liquid particles particularly for case A, (b) Sensitivity study result for (HCl) in the four cases assumed, (c) ClO_x (d) effect on ozone with four different assumptions, where red line indicates Case A, blue line indicates Case B, green line indicates Case C and orange line indicates Case D.

have shown an ozone reformation after the minimum O_3 values were observed. Case B represents the gas phase reaction R18, which is switched off while the heterogeneous reaction R11 takes place on PSCs. In figure 4.4 panel a, the surface area densities of liquid particles, nitric acid trihydrate (NAT) and ice particles are plotted. In case B, gas phase reaction R18 is switched off in the simulation. The effect on the results of the simulation appeared to be in less chlorine activation as compared to case A. Fast chlorine deactivation is observed in figure 4.4 panel b for the case B, C and D, which leads to much slower ozone depletion nearly to the last week of October. The reason for the slow ozone depletion for the three cases B, C and D is indeed the reaction R11 and reaction R18. The role of PSCs is indeed significantly important in ozone hole chemistry. Eventually the NAT and ice particles evaporate due to increase in temperature. Reaction R11 independently has shown a significant impact on the simulated run, as observed in case C. In case C, reaction R11 is switched off resulting in less chlorine activation and faster chlorine deactivation, which has less impact on ozone depletion as compared to case B. Case D represents the importance of both reactions in the ozone depletion process.

4.3 Sensitivity studies

There are still important uncertainties regarding many reactions of relevance to polar ozone chemistry. This regards in particular reactions products, branching ratios and rate constants. To investigate the impact of these uncertainties on the results of our simulations, a range of sensitivity studies has been performed, which are described in this chapter.

4.3.1 Sensitivity study of the reaction between ClO and CH_3O_2 in the gas phase

A new laboratory study by Leather et al. (2012) was conducted which presents the temperature dependent Arrhenius expression for the overall rate constant of reaction R19. The experiment is performed under the influence of temperature and pressure kinetics. The study focuses on the reaction of ClO with CH_3O_2 in the gas phase, which generates two different products methoxy (CH_3O) and methylhypochlorite (CH_3OCl).

$$CH_3O_2 + ClO \rightarrow \text{products} \tag{R50}$$

$$CH_3O_2 + ClO \rightarrow CH_3O + Cl + O_2 \quad \text{(R18)}$$

$$CH_3O_2 + ClO \rightarrow CH_3OCl + O_2(^1\Delta) \quad \text{(R51)}$$

The study is conducted to measure the rate coefficient which is independent of the pressure. The temperature dependent Arrhenius expression with the uncertainties reported by Leather et al. (2012) is given below:

$$k_{10}(T) = (1.96^{+0.28}_{-0.24}) \times 10^{-11} \exp[(-626 \pm 35)/T] \text{cm}^3\text{molecule}^{-1}\text{s}^{-1} \quad (4.1)$$

According to Leather et al. (2012) the impact of the new Arrhenius expression can reduce the effect of ozone loss cycles including reaction R18 in the polar stratosphere by around a factor of 1.5. The Arrhenius value is inserted in the model CLaMS. A comparison between the standard run and the Leather et al. (2012) Arrhenius value is plotted in figure 4.5. The result indicates no significant impact on the model results after replacing the Arrhenius value recommended in Sander et al. (2011b) by the one presented by Leather et al. (2012). In figure 4.5 panel c, the O_3 plot indicates somewhat less depletion as compared to standard run. The O_3 plot is in log scale and the Leather's simulated Arrhenius expression has shown very low ozone values during the early Antarctic spring. No drastic difference between the simulated O_3 values is identified after inserting the Arrhenius value in the CLaMS box-model environment. In figure 4.5 panel a and b shows the mixing ratios of HCl and ClO_x. The product formed in the reaction in this case is assumed to be methoxy (CH_3O) i.e. R18 in the gas phase. In summary, it can be concluded that using the rate constant recommended by Leather et al. (2012) results in no significant change in Antarctic ozone loss chemistry.

4.3.2 Methylhypochlorite (CH_3OCl)

For the net effect of cycle C1 shown in section 4.1 under the heading of standard run, the gas phase reaction between ClO and CH_3O_2 has been shown to be essential. The products of this reaction considered so far are $CH_3O + ClOO$. However, in laboratory experiments (Helleis et al., 1994; Biggs et al., 1995; Tyndall et al., 1998), two reaction

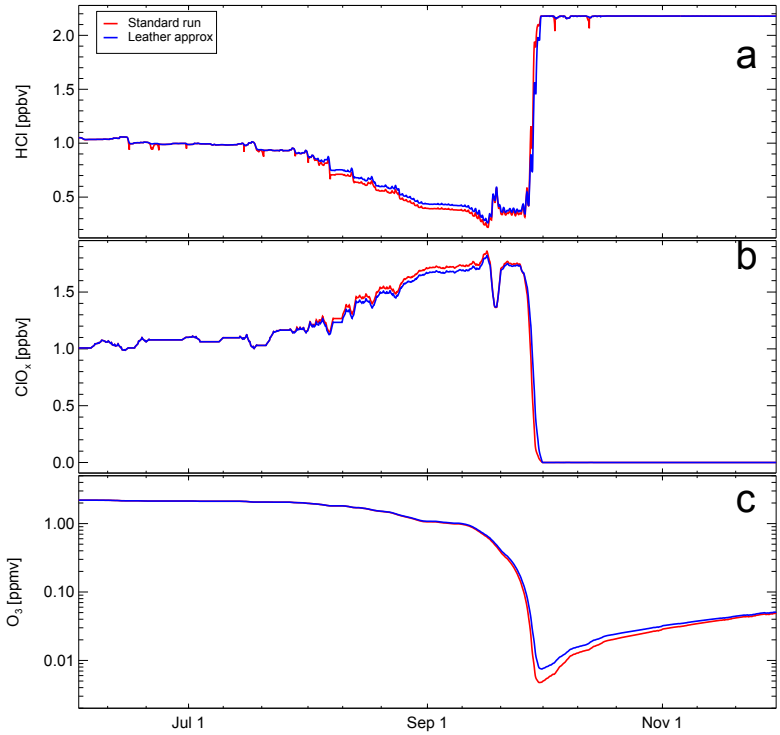

Figure 4.5: Time-series comparison between standard run (red) and simulated results from the Leather et al. (2012) Arrhenius expression (blue) representing the panels (a) HCl, (b) ClO_x and (c) O_3.

channels have been identified for the reaction $CH_3O_2 + ClO$:

$$CH_3O_2 + ClO \rightarrow \text{products} \quad \text{(R50)}$$

$$CH_3O_2 + ClO \rightarrow CH_3O + ClOO \quad \text{(R18)}$$

$$CH_3O_2 + ClO \rightarrow CH_3OCl + O_2 \quad \text{(R51)}$$

According to Helleis et al. (1994), the two production channels from the reaction $CH_3O_2 + ClO$ favour the partition of approximately 77% into methoxy (CH_3O) while 23% into methylhypochlorite (CH_3OCl). In the model the formation of methylhypochlorite is introduced and loss of CH_3OCl happens due to photolysis, which is an important removal process for CH_3OCl. The loss of methylhypochlorite (CH_3OCl) through photolysis has been shown in the figure 4.6 in blue line.

$$CH_3OCl + h\nu \rightarrow CH_3O + Cl \quad \text{(R52)}$$

(Crowley et al., 1994), whereas reaction of CH_3OCl with OH is negligible (Crowley et al., 1996). The net result of reactions 51 and 52 is:

$$\begin{aligned} & CH_3O_2 + ClO \rightarrow CH_3OCl + O_2 && \text{(R51)} \\ & CH_3OCl + h\nu \rightarrow CH_3O + Cl && \text{(R52)} \\ \textit{Net}: \quad & CH_3O_2 + ClO \rightarrow CH_3O + Cl + O_2 \end{aligned}$$

The net effect is same as reaction R18, so that cycle C1 remains unaltered. Indeed, the results of a simulation assuming 100% formation of CH_3OCl in reaction R51 and photolysis of CH_3OCl as in reaction R52 is the only loss process, results in a very similar behaviour of chlorine activation and ozone loss, blue line in figure 4.6 as in the reference run.

Reaction with Cl

Carl et al. (1996) and Kukui et al. (1997) introduced a further relevant reaction pathway for methylhypochlorite (CH_3OCl), namely the reaction with Cl and reported rate

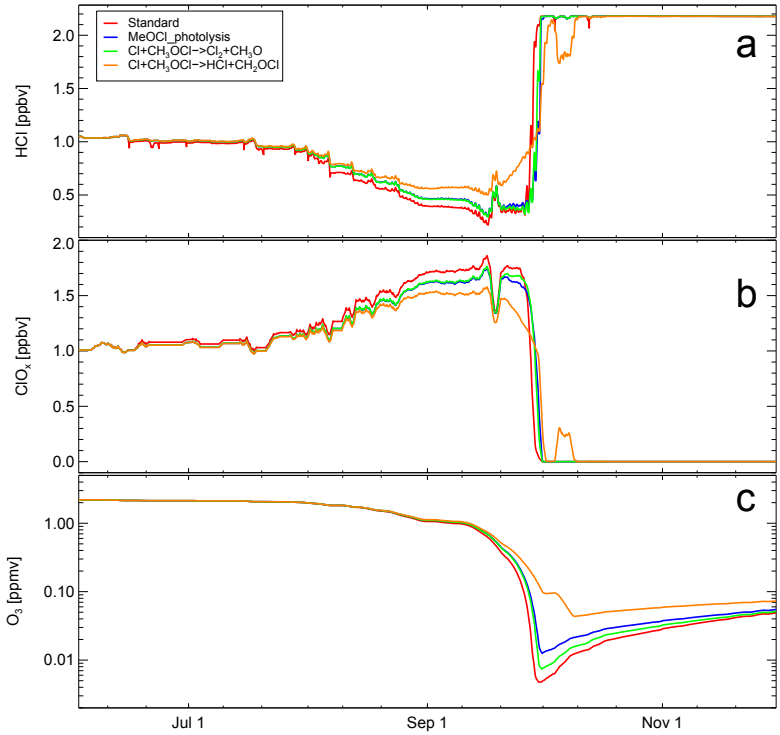

Figure 4.6: Time series for the sensitivity study of methylhypochlorite (CH_3OCl) performed. Red line indicates the standard case as a base run (see figure 4.1), blue line indicates the loss of CH_3OCl through photolysis (see reaction R52), green line presents the reaction of methylhypochlorite (CH_3OCl) with Cl resulting in Cl_2 production reported by Helleis et al. (1994), and orange line represents the HCl production from the partition reaction of methylhypochlorite (CH_3OCl) with Cl according to Helleis et al. (1994), with the reaction products given in the legend in panel a.

constants and reaction products:

$$CH_3OCl + Cl \rightarrow CH_3O + Cl_2 \quad \text{(R53)}$$

$$CH_3OCl + Cl \rightarrow CH_2OCl + HCl \quad \text{(R54)}$$

where CH_2OCl rapidly reacts further via (Carl et al., 1996):

$$CH_2OCl \rightarrow CH_2O + Cl \quad \text{(R55)}$$

Reaction R53 constitutes the dominant pathway (about 85%, Carl et al. (1996); Kukui et al. (1997)) and leads to the following sequence:

$$\begin{aligned}
& CH_3O_2 + ClO \rightarrow CH_3OCl + O_2 && \text{(R51)}\\
& CH_3OCl + Cl \rightarrow CH_3O + Cl_2 && \text{(R53)}\\
& Cl_2 + h\nu \rightarrow 2\,Cl && \text{(R7)}\\
& Cl + O_3 \rightarrow ClO + O_2 && \text{(R4)}\\
& CH_3O + O_2 \rightarrow CH_2O + HO_2 && \text{(R56)}\\
Net: \quad & CH_3O_2 + ClO \rightarrow CH_2O + HO_2 + Cl &&
\end{aligned}$$

The net production of methylhypochlorite (CH_3OCl) has shown no significant effect on the production of formaldehyde (CH_2O). Comparing blue line and green line in figure 4.6, the case in which photolysis of methylhypochlorite is assumed as loss process. The loss of methylhypochlorite is fast through photolysis rather than gas phase loss reaction i.e. R53. The minor reaction pathway R18 leads to the net reaction:

$$CH_3O_2 + ClO \rightarrow CH_2O + HCl + O_2 \quad \text{(R57)}$$

and thus to a net deactivation of chlorine. The green line represents the reaction R53 in figure 4.6. The green line and blue line are almost identical in the figure 4.6, the major loss process in both simulation is CH_3OCl photolysis. In figure 4.6 green line, excess Cl_2 is generated which could effect the cycle C1 but not enough to create a significant effect. However, a run assuming additional HCl production in reaction R57 (orange line in figure 4.6) shows a larger difference to the reference run. In figure 4.6 the orange line shows the case for which enhanced HCl is generated in reaction R57. Again, the loss of

CH_3OCl is assumed through photolysis in this simulation (orange line). Reaction R57 is assumed to generate HCl and CH_2O. Since under these conditions no HO_2 is formed in R57, this slows down cycle C1. Thus the simulated results show a slow activation of chlorine and thus lower ClO_x, which results in ozone loss delayed by two weeks.

Heterogeneous reaction

Kenner et al. (1993) and Crowley et al. (1994) suggested that the heterogeneous reaction

$$CH_3OCl + HCl \rightarrow CH_3OH + Cl_2 \qquad \text{(R58)}$$

might take place in analogy with the heterogeneous reaction R11. If this reaction occurred in the polar stratosphere, it would constitute a significant source of methanol (CH_3OH). Assuming that reaction R58 takes place it should lead to the following reaction sequence:

$$\begin{aligned}
& CH_3O_2 + ClO \rightarrow CH_3OCl + O_2 && \text{(R51)}\\
& CH_3OCl + HCl \rightarrow CH_3OH + Cl_2 && \text{(R58)}\\
& Cl_2 + h\nu \rightarrow 2\,Cl && \text{(R7)}\\
& Cl + O_3 \rightarrow ClO + O_2 && \text{(R4)}\\
& CH_3OH + Cl \rightarrow HCl + CH_3O && \text{(R59)}\\
& CH_3O + O_2 \rightarrow CH_2O + HO_2 && \text{(R60)}\\
\textit{Net}: \quad & CH_3O_2 + ClO \rightarrow CH_2O + HO_2 + Cl &&
\end{aligned}$$

Thus, again, the net effect of this cycle is producing the same products as reaction R18 directly. In figure 4.7, it is observable that addition of the heterogeneous reaction R58 into model could not produce the significant effect on the ozone loss. However, the HCl in panel a, has shown somewhat less activation as compared to the reference run. And HCl deactivation (rapid increase) is delayed by one or one and a half day. It is evident that the more HCl being produced i.e. a reservoir species of activated chlorine will lead to less ozone depletion. Nonetheless the ozone loss is strong enough for the ozone values to reach the minimum ozone mixing ratios.

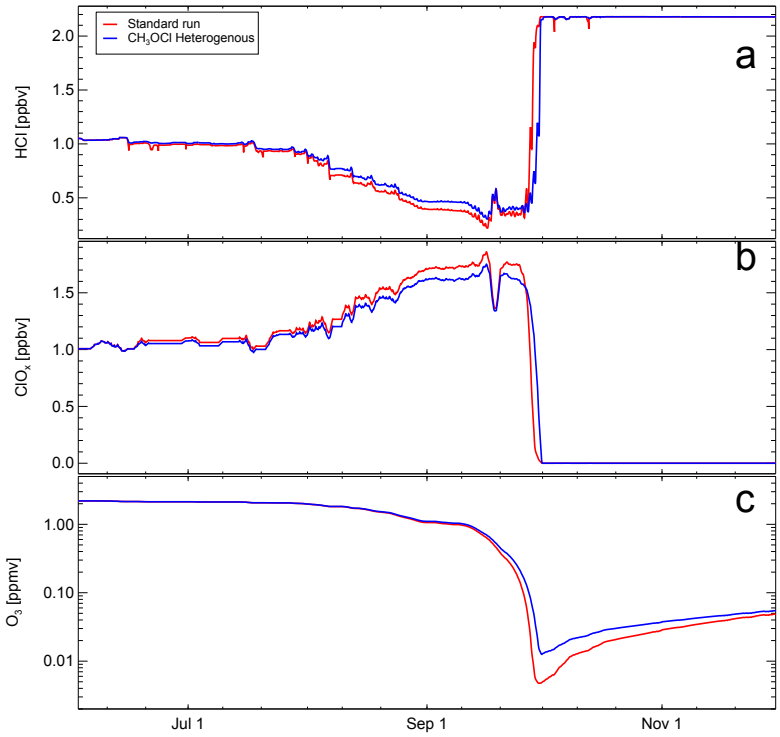

Figure 4.7: Sensitivity study for methylhypochlorite (CH_3OCl) reacting heterogeneously on ice, NAT and liquid surfaces. Where red line indicates the reference run and blue line indicates the simulated result of CH_3OCl reacting heterogeneously.

4.4 Importance of formaldehyde (CH_2O) photolysis

The formaldehyde photolysis plays a key role in the ozone hole chemistry. The HCl decrease which is discussed in detail in the section 4.1, requires HO_2 formation beyond the production in reactions R19 and R49. In section 4.1, the two cycles C1 and C2 are representing the methane oxidation, but these two cycles could neither explain the decrease in HCl nor the complete activation of chlorine as observed (Santee et al., 2008).

Under the conditions in the polar lower stratosphere in the late winter and early spring the production of O^1D radicals reacting with H_2O is not the dominant source for the formation of HO_x radicals. But, the production of formaldehyde (CH_2O) leads to HO_x formation through CH_2O oxidation.

$$CH_2O + h\nu \rightarrow HCO + H \quad \text{(R47)}$$

$$H + O_2 \rightarrow HO_2 \quad \text{(R61)}$$

$$CHO + O_2 \rightarrow CO + 2\,HO_2 \quad \text{(R62)}$$

$$Net: \quad CH_2O + 2O_2 \rightarrow CO + 2HO_2 \quad \text{(R63)}$$

The photolysis of formaldehyde consists on two channels; reaction R47 leading to the formation of two HO_2 radicals and the molecular channel

$$CH_2O + h\nu \rightarrow H_2 + CO \quad \text{(R46)}$$

which does not lead to the production of HO_x. The branching ratio between reactions R47 and R46 is variable and is about 30% for channel R47 in the late August and early September. To distinguish the importance of reaction channels between R47 and R46, a sensitivity run was introduced with the extreme assumption of 100% efficiency for each channel. In this case the other channel is stopped to take part in the run (e.g. reaction R47 [red line] is assumed at 100% efficiency and reaction R46 [blue line] is assumed to be zero; see figure 4.8). In figure 4.8, it is evident that reaction R47 produces more HO_2 resulting in faster HCl reduction and nearly zero values of HCl in the month of August as compared to the standard run. Consequently, higher ClO_x is obtained which results in fast ozone depletion. Meanwhile, faster ozone loss is obtained earlier than in the standard run and similarly, the rapid HCl increase has been observed in the figure 4.8 [red line]. Moreover, in the other run where the assumption of no HO_2 formation in the CH_2O oxidation is made, the results are totally different. Much less HCl decrease

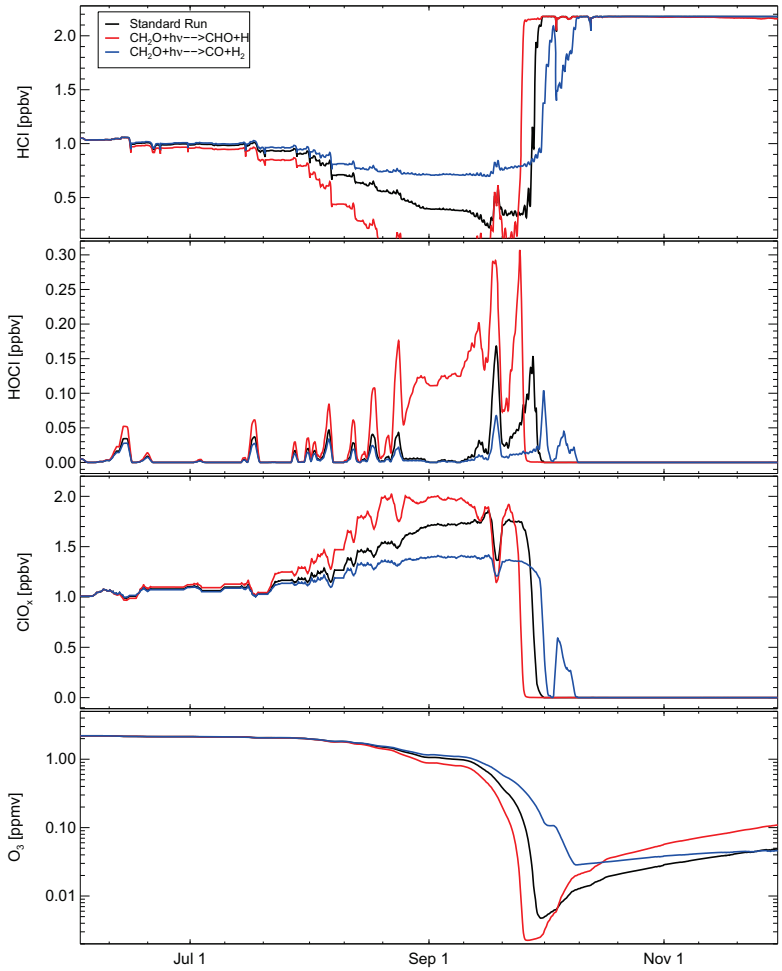

Figure 4.8: Sensitivity study of formaldehyde (CH_2O) performed. Red line indicates the reaction R47 channel contributing in the production of HO_2 with the 100% efficiency and blue line represents 100% efficiency of the molecular channel R46 with no HO_2 production.

is simulated resulting in low chlorine activation, i.e. low ClO_x and in accordance with less activation much less ozone depletion occurs (blue line in figure 4.8).

4.4.1 A new quantum yield expression for CH_2O photolysis

Röth and Ehhalt (2015) reported a new expression for the wavelength-dependent photolysis quantum yields of CH_2O, ϕ_j. The calculated quantum yield is based on the data currently recommended by JPL (Sander et al., 2011a) and IUPAC. The photolysis of formaldehyde includes two reaction channels R46 and R47. The quantum yield is being calculated for both the radical and molecular channel. The total quantum yield is defined as $\phi_{\text{total}}=\phi_{\text{rad}}+\phi_{\text{mol}}$. Where ϕ_{rad} belongs to reaction R47 and ϕ_{mol} belongs to reaction R46 in the model. Röth and Ehhalt (2015) calculated the total quantum yield and the quantum yield for each radical channel. The molecular channel is driven by the difference between total and radical quantum yields. The expression (for λ in nm) presented by Röth and Ehhalt (2015) is given below:

$$\Phi_{\text{rad}} = \frac{0.74 \pm 0.01}{1+\exp(\frac{-(1/\lambda - 1/327.4 \pm 0.5)}{(5.4\pm0.5)\times10^{-5}})} - \frac{0.40 \pm 0.04}{1+\exp(\frac{-(1/\lambda - 1/279.0 \pm 1.3)}{(5.2\pm2.4)\times10^{-5}})} \tag{4.2}$$

$$\Phi_{\text{tot}} = \frac{1}{1+\exp(\frac{-(1/\lambda - 1/346.9 \pm 0.5)}{(5.4\pm0.3)\times10^{-5}})(\frac{M}{M_0})} - \frac{0.22 \pm 0.02}{1+\exp(\frac{-(1/\lambda - 1/279.0 \pm 1.3)}{(5.2\pm2.4)\times10^{-5}})} \tag{4.3}$$

from the above two equations 4.2 and 4.3, molecular quantum yield can be calculated as shown below:

$$\begin{aligned}\Phi_{\text{mol}} \quad = \quad & \frac{1}{1+\exp(\frac{-(1/\lambda - 1/346.9 \pm 0.5)}{(5.4\pm0.3)\times10^{-5}})(\frac{M}{M_0})} - \frac{0.74 \pm 0.01}{1+\exp(\frac{-(1/\lambda - 1/327.4 \pm 0.5)}{(5.4\pm0.5)\times10^{-5}})} \\ & + \frac{0.18 \pm 0.02}{1+\exp(\frac{-(1/\lambda - 1/279.0 \pm 1.3)}{(5.2\pm2.4)\times10^{-5}})}\end{aligned} \tag{4.4}$$

Equations 4.2 and 4.4 were added to the model to compare the effect of calculated quantum yields with the JPL recommendations, which are used in the model. The effect on the model is not significant, the black line in figure 4.9 indicates the reference run based on the JPL recommended quantum yields, and red line indicates the modified quantum yields suggested by Röth and Ehhalt (2015). The red and the black line are almost identical.

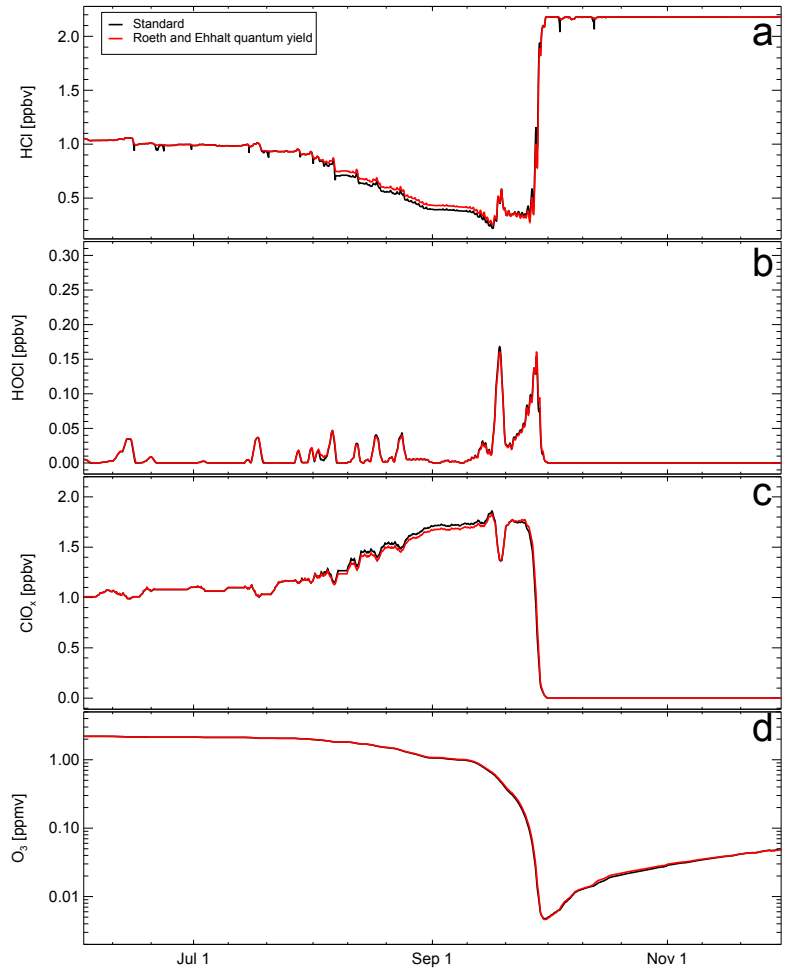

Figure 4.9: Reference run indicates in a black line with the addition of Röth and Ehhalt (2015) quantum yield expression in the model (Red line).

4.5 Sensitivity of Antarctic ozone loss on Stratospheric methane and chlorine

Because of the success of Montreal Protocol (UNEP, 1987) and its amendments and adjustments, the halogen loading in the stratosphere will decrease in the coming decades. Thus, the composition of the Antarctic lower stratosphere will change subsequently. To assess the impact of the expected decrease in the halogen loading on Antarctic ozone loss by the mid of this century, we introduced two additional sensitivity runs based on the standard run as a reference. Total chlorine Cl_y (Cl_y here, represents the mixing ratios of $HCl, ClONO_2, HOCl, ClO, Cl_2O_2$ and Cl_2) is reduced to half because chlorine is the most abundant halogen element in the atmosphere; we reduced chlorine by initiating the sensitivity run with half the amount of Cl_y. As in the future, CH_4 is expected to increase in the stratosphere, the CH_4 value is increased to twice the value assumed for the reference run. As an additional run, both assumptions of increasing the value of methane (CH_4) as twice and halved the Cl_y are combined together. The run with Cl_y reduced to half (blue line in the figure 4.10) results in lower chlorine activation and similarly slower ozone loss rates. In figure 4.10 panel e, the ozone plot for the halved Cl_y shows consequently a delayed ozone depletion, but still very low values for ozone are reached (minimum around ≈ 0.2 ppb). In comparison with the standard run, the low values of ozone depletion for halved Cl_y are delayed by three weeks. The model setup is similar for the halved Cl_y instead of assuming the initial concentration of Cl_y to be halved. The ozone values are reaching low enough in the halved Cl_y assumption, but the delay in reaching the low values is due to a slower ozone loss rate which is caused by the lower Cl_y values.

On the other hand the assumption of doubling the initial mixing ratio of methane (CH_4) leads to a speed up the reaction R10 but does not lead to modified deactivation of chlorine (as one might have intuitively expected), because cycles C1 and C2 are active and inhibit the deactivation effect of reaction R10. Doubling methane would result in faster chlorine activation because of the increase in production of formaldehyde CH_2O in cycle C1. And the HCl activation starts from the end of August and early September and resulting in higher ClO_x and faster ozone depletion during this period.

In the run when both the above conditions are assumed together (i.e. Doubling the methane and half of Cl_y) presented in green colour in figure 4.10, the results did not show a significant effect in deactivation of chlorine. Very low ozone values are reached still in the month of October. From this run it can be concluded that very low ozone

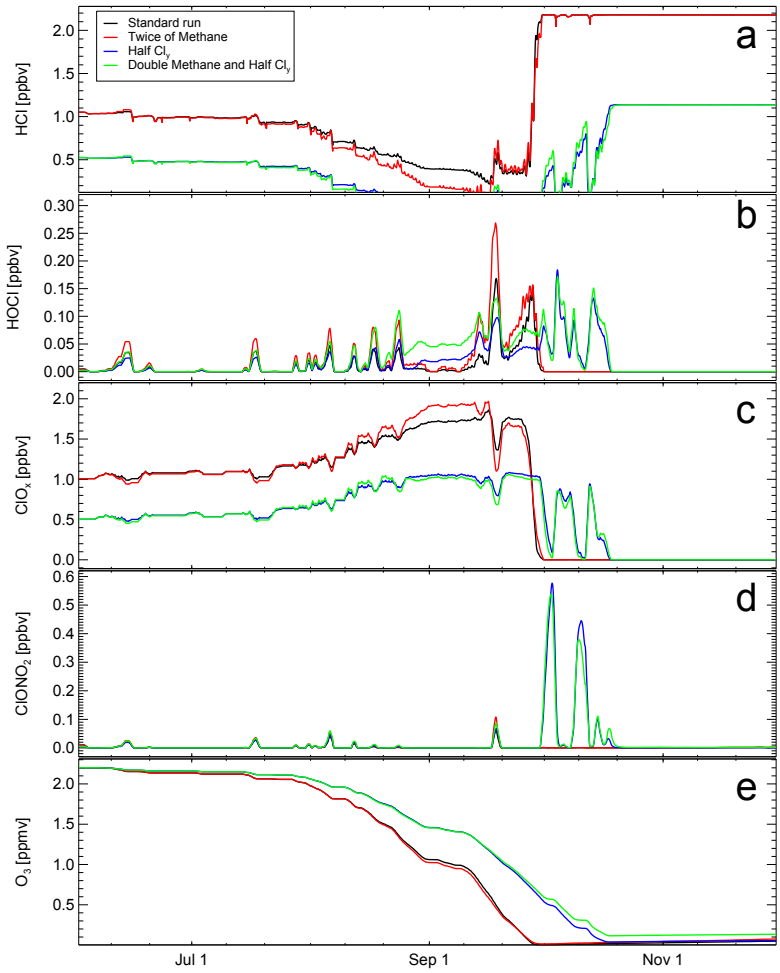

Figure 4.10: A figure corresponding to the future prediction representing standard run (black line), simulation on doubling the concentration of methane CH_4 (red line), a simulated result for half of the initial chlorine Cl_y in blue, and a future prediction of combining the both assumption together with twice of methane and half chlorine initial concentration is presented in green line.

mixing ratios will still be present in the Antarctic stratosphere, even though the chlorine loading is significantly reduced. However, the ozone hole appearance will be delayed by three weeks for the lowest ozone mixing ratios.

4.6 Sensitivity on initial Ozone concentrations

In this section, sensitivity simulations on initial ozone concentrations in the model results are described. For these box-model simulations, a model setup is used similar to the reference run but with different initial ozone mixing ratios. Figure 4.11, shows six additional runs performed on the similar model setup but with different initial ozone mixing ratios, in which four initial mixing ratios are set to increase in increments of 0.1 ppmv. The initial value in the reference run used for ozone is 2.20 ppmv and the highest ozone mixing ratio value used in these runs reached 2.6 ppmv. Two additional runs were performed with the assumption of lower initial ozone mixing ratios from the present values of ozone, which is not a realistic scenario, as in the future, ozone will increase in stratosphere. For the low initial ozone mixing ratios, which is an unrealistic case, we assumed the values of 2.10 and 2.00 ppmv. In the cases shown in figure

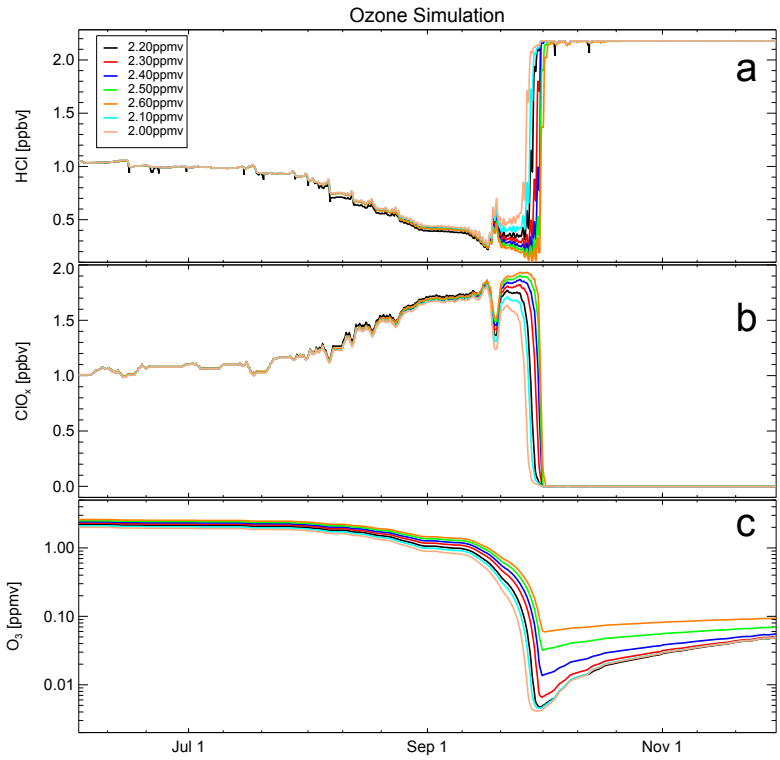

Figure 4.11: Simulation run for different ozone mixing ratios. Black line indicates the standard run.

4.11, the trajectories are identical to the reference run. The resulting behaviour of the chemistry is similar as in the reference run. The reservoir species HCl is activated into ClO_x. Hence, minimum ozone mixing ratios observed are similar to reference run. The

chlorine deactivation i.e. increase in HCl shifts in time depending upon the different ozone mixing ratios. In the 2.60 ppmv initial ozone mixing ratio simulation, chlorine activation is maximum, which delayed the lowest possible ozone mixing ratio but still very low ozone mixing ratios are observed. Nonetheless, for 2.60 ppmv initial ozone, there is more ozone to be destroyed so it takes longer to reach extremely low values. In the 2.60 ppmv initial ozone case, in the beginning of October (3rd of October precisely) PSCs disappear due to higher temperatures (above $\approx$195 K) which causes cycles C1 and C2 (see page number 37) to stop because of the halt of reaction R11. This leads to increasing HCl, which disrupts the ozone depletion. The reason is the unavailability of PSCs due to higher temperatures above than 195K by the beginning of the month of October. Slow ozone loss rates shifted very low ozone mixing ratios in the 2.60 ppmv simulation (orange line) because ozone was available in sufficient quantity.
Similarly, for the lowest initial ozone mixing ratio (2.00 ppmv), the chlorine activation is less as ozone is not available for cycles C1 and C2 to proceed. Ozone is so low that minimum ozone is reached before 1st of October, which is low enough to cause cycles C1 and C2 (see page number 37) to stop, thus HCl to increase and O_3 loss stop.

5 Summary and Conclusion

In this thesis, several key chemical processes have been discussed that are responsible for Antarctic ozone depletion in the core of the polar vortex in the lower stratosphere. The model employed here is based on a single air parcel in box model environment, where the trajectory intersects the South pole ozone sonde observation on 24^{th} of September. The employed model is CLaMS in a setup similar as in the study by Grooß et al. (2011), however, the model is operated here assuming low NAT number densities in contrast to the assumptions by Grooß et al. (2011).

We find that, in contrast to common belief, the formation of HCl in the reactions $CH_2O + Cl$ and $CH_4 + Cl$ does not lead to deactivation of chlorine during the period of strongest ozone destruction. This is the case because two reaction cycles (C1 and C2, see page 37) contribute to reactivation of chlorine involving the heterogeneous reaction (i.e. $HOCl + HCl$) as long as some ozone is still present. The lowest ozone mixing ratios ($\approx$ 10 ppbv) achieved in the box model simulation are comparable to ozone sonde observations. At these extremely low ozone mixing ratios, the before mentioned cycles come to a halt which triggers the deactivation of activated chlorine (ClO_x) into HCl rapidly. The ozone depletion stops once the low ozone mixing ratios are reached, even in the presence of PSCs and low temperatures because chlorine is rapidly deactivated.

Extensive sensitivity studies were performed using the CLaMS box model. Firstly, we revised the study of Crutzen et al. (1992), which was focused on the importance of gas phase ($CH_3O_2 + ClO$) reaction and heterogeneous phase ($HOCl + HCl$) reaction. A significant impact of these reactions was found similar to the old study. Secondly, formaldehyde (CH_2O) photolysis was tested in the model and it is concluded that HO_x production from CH_2O photolysis is essential for the complete depletion of HCl (and thus for the complete activation of Cl) through the formation of HOCl. Few laboratory studies were reporting the production of methylhypochlorite (CH_3OCl), sensitivity tests were performed according to the studies (Helleis et al., 1994; Biggs et al., 1995; Tyndall et al., 1998) reporting branching ratios of the formation of CH_3OCl in the reaction $CH_3O_2 + ClO$. We find that including (CH_3OCl) in the reaction scheme does not lead

to significant changes in the reaction cycles discussed above, so that conclusions regarding the importance of the reaction $CH_3O_2 + ClO$ remain unchanged. In the future, increase in the greenhouse gases methane (CH_4) and lower chlorine loadings in stratosphere will affect the stratospheric composition. Based on this fact, a sensitivity study was performed keeping in mind that ozone will increase according to WMO (2014) report due to decrease in EESC. We find that increasing methane will not substantially affect polar ozone chemistry in the Antarctic and that extremely low ozone values will still occur even for half of the current stratospheric chlorine loading albeit about two weeks later in the season.

In conclusion, the study helped to understand the activation and deactivation of chlorine under Antarctic ozone hole conditions. The model calculated low ozone values approximately reaching 10 ppbv. This corroborates that our model calculations and ozone sonde observations are in close agreement regarding very low ozone values during winter and spring season at South pole. Further, ozone loss will continue to happen in next few decades; it will certainly slow down in the future, but it is difficult to quantify exactly when it will stop. There are still open questions regarding the polar vortex chemistry.

5.1 Outlook

In this study, model is set up for a simple box model analysis. This study allows a detailed analysis of the chemical mechanisms, but should be extended into a three dimensional model study for a better representation of the polar vortex. Mixing of air parcels is neglected in the case presented here, but in 3-d environment mixing of air parcels can be assumed as an example of reality in the polar vortex mechanisms including dynamics.

Considering one air parcel cannot explain every mechanism in the polar vortex chemistry. For further understanding of the single air parcel, we have initiated a collaboration with R. Lehmann (Alfred Wegener Institut, Potsdam), who introduced an algorithm to determine the pathways for significant chemical reactions during the period of the ozone hole (Lehmann, 2004). The purpose of Lehmann's analysis will be to figure out and quantify the key reactions involved in deactivation of chlorine.

References

Abbatt, J. P. D. and Molina, M. J.: Heterogeneous interactions of $ClONO_2$ and HCl on nitric acid trihydrate at 202 K, J. Phys. Chem., 96, 7674–7679, 1992.

Anderson, J. G., Toohey, D. W., and Brune, W. H.: Free Radicals Within the Antarctic Vortex: The Role of CFCs in Antarctic Ozone Loss, Science, 251, 39–46, 1991.

Becker, G., Grooß, J.-U., McKenna, D. S., and Müller, R.: Stratospheric photolysis frequencies: Impact of an improved numerical solution of the radiative transfer equation, J. Atmos. Chem., 37, 217–229, doi:10.1023/A:1006468926530, 2000.

Biggs, P., Canosa-Mas, C. E., Fracheboud, J.-M., Shallcross, D. E., and Wayne, R. P.: Efficiency of formation of CH_3O in the reaction of CH_3O_2 with ClO, Geophys. Res. Lett., 22, 1221–1224, doi:10.1029/95GL01011, 1995.

Brown, P. N., Byrne, G. D., and Hindmarsh, A. C.: VODE: A variable coefficient ODE solver, SIAM J. Sci. Stat. Comput., 10, 1038–1051, 1989.

Carl, S. A., Roehl, C. M., Müller, R., Moortgat, G. K., and Crowley, J. N.: Rate Constant and Mechanism of The Reaction Between Cl and CH_3OCl at 295 K, J Phys Chem, 106, 17 191–17 201, 1996.

Carslaw, K. S. and Peter, T.: Uncertainties in reactive uptake coefficients for solid stratospheric particles - 1. Surface chemistry, Geophys. Res. Lett., 24, 1743–1746, 1997.

Carver, G. D., Brown, P. D., and Wild, O.: The ASAD atmospheric chemistry integration package and chemical reaction database, Computer Physics Communications, 105, 197–215, 1997.

Crowley, J. N., Helleis, F., Müller, R., Moortgat, G. K., Crutzen, P. J., and Orlando, J. J.: CH_3OCl: UV/Vis absorption cross-sections, J values and atmospheric significance, J. Geophys. Res., 99, 20 683–20 688, 1994.

Crowley, J. N., Campuzano-Jost, P., and Moortgat, G. K.: Temperature dependent rate constants for the gas-phase reaction between OH and CH_3OCl, J. Phys. Chem., 100, 3601–3606, 1996.

Crutzen, P. J.: Estimates of possible future ozone reductions from continued use of fluro-chloro-methanes (CF_2Cl_2, $CFCl_3$), Geophys. Res. Lett., 1, 205–208, 1974.

Crutzen, P. J., Müller, R., Brühl, C., and Peter, T.: On the potential importance of the gas phase reaction $CH_3O_2 + ClO \rightarrow ClOO + CH_3O$ and the heterogeneous reaction $HOCl + HCl \rightarrow H_2O + Cl_2$ in "ozone hole" chemistry, Geophys. Res. Lett., 19, 1113–1116, doi:10.1029/92GL01172, 1992.

Daniel, J. S., Solomon, S., and Albritton, D. L.: On the evaluation of halocarbon radiative forcing and global warming potentials, J. Geophys. Res., 100, 1271–1285, doi:10.1029/94JD02516, 1996.

Dee, D. P., Uppala, S. M., Simmons, A. J., Berrisford, P., Poli, P., Kobayashi, S., Andrae, U., Balmaseda, M. A., Balsamo, G., Bauer, P., Bechtold, P., Beljaars, A. C. M., van de Berg, L., Bidlot, J., Bormann, N., Delsol, C., Dragani, R., Fuentes, M., Geer, A. J., Haimberger, L., Healy, S. B., Hersbach, H., Hólm, E. V., Isaksen, L., Kållberg, P., Köhler, M., Matricardi, M., McNally, A. P., Monge-Sanz, B. M., Morcrette, J.-J., Park, B.-K., Peubey, C., de Rosnay, P., Tavolato, C., Thépaut, J.-N., and Vitart, F.: The ERA-Interim reanalysis: configuration and performance of the data assimilation system, Q. J. R. Meteorol. Soc., 137, 553–597, doi:10.1002/qj.828, 2011.

Dobson, G. M. B. and Harrison, D. N.: Measurements of the amount of ozone in the Earth's atmosphere and its relation to other geophysical conditions, Proc. R. Soc. London A, 110, 660–693, 1926.

Douglass, A. R., Schoeberl, M. R., Stolarski, R. S., Waters, J. W., Russell III, J. M., Roche, A. E., and Massie, S. T.: Interhemispheric differences in springtime production of HCl and $ClONO_2$ in the polar vortices, J. Geophys. Res., 100, 13 967–13 978, 1995.

Drdla, K. and Müller, R.: Temperature thresholds for chlorine activation and ozone loss in the polar stratosphere, Ann. Geophys., 30, 1055–1073, doi:10.5194/angeo-30-1-2012, 2012.

Farman, J. C., Gardiner, B. G., and Shanklin, J. D.: Large losses of total ozone in Antarctica reveal seasonal ClO_x/NO_x interaction, Nature, 315, 207–210, 1985.

Grooß, J.-U. and Russell, J. M.: Technical note: A stratospheric climatology for O_3, H_2O, CH_4, NO_x, HCl, and HF derived from HALOE measurements, Atmos. Chem. Phys., 5, 2797–2807, 2005.

Grooß, J.-U., Pierce, R. B., Crutzen, P. J., Grose, W. L., and Russell III, J. M.: Reformation of chlorine reservoirs in southern hemisphere polar spring, J. Geophys. Res., 102, 13 141–13 152, doi:10.1029/96JD03505, 1997.

Grooß, J.-U., Konopka, P., and Müller, R.: Ozone chemistry during the 2002 Antarctic vortex split, J. Atmos. Sci., 62, 860–870, 2005.

Grooß, J.-U., Brautzsch, K., Pommrich, R., Solomon, S., and Müller, R.: Stratospheric ozone chemistry in the Antarctic: What controls the lowest values that can be reached and their recovery?, Atmos. Chem. Phys., 11, 12 217–12 226, 2011.

Grooß, J.-U., Engel, I., Borrmann, S., Frey, W., Günther, G., Hoyle, C. R., Kivi, R., Luo, B. P., Molleker, S., Peter, T., Pitts, M. C., Schlager, H., Stiller, G., Vömel, H., Walker, K. A., and Müller, R.: Nitric acid trihydrate nucleation and denitrification in the Arctic stratosphere, Atmos. Chem. Phys., 14, 1055–1073, doi:10.5194/acp-14-1055-2014, 2014.

Hanson, D. R. and Ravishankara, A. R.: The reaction probabilities of $ClONO_2$ and N_2O_5 on 40 to 75% sulfuric acid solutions, J. Geophys. Res., 96, 17 307–17 314, 1991.

Hanson, D. R. and Ravishankara, A. R.: Investigation of the reactive and nonreactive processes involving $ClONO_2$ and HCl on water and nitric-acid doped ice, J. Phys. Chem., 96, 2682–2691, 1992.

Hanson, D. R. and Ravishankara, A. R.: Reaction of $ClONO_2$ with HCl on NAT, NAD, and frozen sulfuric acid and hydrolysis of N_2O_5 and $ClONO_2$ on frozen sulfuric acid, J. Geophys. Res., 98, 22 931–22 936, 1993.

Helleis, F., Crowley, J. N., and Moortgat, G. K.: Temperature dependent CH_3OCl formation in the reaction between CH_3O_2 and ClO, Geophys. Res. Lett., 21, 1795–1798, doi:10.1029/94GL01280, 1994.

Jones, A. E. and Shanklin, J. D.: Continued decline of total ozone over Halley, Antarctica, since 1985, Nature, 376, 409–411, 1995.

Kawa, S. R., Stolarski, R. S., Newman, P. A., Douglass, A. R., Rex, M., Hofmann, D. J., Santee, M. L., and Frieler, K.: Sensitivity of polar stratospheric ozone loss to uncertainties in chemical reaction kinetics, Atmos. Chem. Phys., 9, 8651–8660, doi:10.5194/acp-9-8651-2009, 2009.

Kenner, R. D., Ryan, K. R., and Plumb, I. C.: Kinetics of the reaction of CH_3O_2 with ClO at 293 K, Geophys. Res. Lett., 20, 1571–1574, 1993.

Konopka, P., Steinhorst, H.-M., Grooß, J.-U., Günther, G., Müller, R., Elkins, J. W., Jost, H.-J., Richard, E., Schmidt, U., Toon, G., and McKenna, D. S.: Mixing and Ozone Loss in the 1999-2000 Arctic Vortex: Simulations with the 3-dimensional Chemical Lagrangian Model of the Stratosphere (CLaMS), J. Geophys. Res., 109, D02315, doi:10.1029/2003JD003792, 2004.

Kukui, A., Roggenbuck, J., and Schindler, R.: Mechanism and rate constants for the reactions of Cl atoms with HOCl, CH_3OCl and tert-C_4H_9OCl, Ber. Bunsenges. Phys. Chem., 101, 281–286, 1997.

Lary, D. J., Chipperfield, M. P., Toumi, R., and Lenton, T.: Heterogeneous Atmospheric Bromine Chemistry, J. Geophys. Res., 101, 1489–1504, 1996.

Leather, K. E., Bacak, A., Wamsley, R., Archibald, A. T., Husk, A., Shallcross, D. E., and Percival, C. J.: Temperature and pressure dependence of the rate coefficient for the reaction between ClO and CH_3O_2 in the gas-phase, Phys. Chem. Chem. Phys., 14, 3425–3434, doi:10.1039/C2CP22834C, 2012.

Lehmann, R.: An algorithm for the determination of all significant pathways in chemical reaction systems, J. Atmos. Chem., 47, 45–78, 2004.

Lovelock, J. E., Maggs, R., and Wade, R.: Halogenated hydrocarbons in and over the Atlantic, Nature, 241, 194–196, 1973.

McElroy, M. B., Salawitch, R. J., Wofsy, S. C., and Logan, J. A.: Antarctic ozone: Reductions due to synergistic interactions of chlorine and bromine, Nature, 321, 759–762, 1986.

McKenna, D. S., Grooß, J.-U., Günther, G., Konopka, P., Müller, R., Carver, G., and Sasano, Y.: A new Chemical Lagrangian Model of the Stratosphere (CLaMS): 2. Formulation of chemistry scheme and initialization, J. Geophys. Res., 107, 4256, doi:10.1029/2000JD000113, 2002a.

McKenna, D. S., Konopka, P., Grooß, J.-U., Günther, G., Müller, R., Spang, R., Offermann, D., and Orsolini, Y.: A new Chemical Lagrangian Model of the Stratosphere (CLaMS): 1. Formulation of advection and mixing, J. Geophys. Res., 107, 4309, doi:10.1029/2000JD000114, 2002b.

Meier, R. R., Anderson, D. E., J., and Nicolet, M.: Radiation Field in the Troposphere and Stratosphere from 240-1000 nm -I: General Analysis, Planet Space Sci, 30, 923–933, 1982.

Molina, L. T. and Molina, M. J.: Production of Cl_2O_2 from the self-reaction of the ClO radical, J. Phys. Chem., 91, 433–436, 1987.

Molina, M. J. and Rowland, F. S.: Stratospheric sink for chlorofluoromethanes: chlorine atom catalysed destruction of ozone, Nature, 249, 810–812, 1974.

Montzka, S.: Stratospheric Ozone Depletion and Climate Change, chap. Source gases that affect stratospheric ozone, pp. 33–77, The Royal Society of Chemistry, 2012.

Morcrette, J.-J.: Radiation and Cloud Radiative Properties in the European Centre for Medium-Range Weather Forecasts Forecasting System, J. Geophys. Res., 96, 9121–9132, 1991.

Müller, R.: A brief history of stratospheric ozone research, Meteorol. Z., 18, 3–24, doi:10.1127/0941-2948/2009/353, 2009.

Müller, R.: Tracer-tracer relations as tool for research on polar ozone loss, vol. 58 of *Schriften des Forschungszentrums Jülich, Reihe Energie & Umwelt*, Forschungszentrum Jülich, Jülich, 2010.

Müller, R.: Introduction, in: Stratospheric Ozone Depletion and Climate Change, edited by Müller, R., pp. 1–32, Royal Society of Chemistry, doi:10.1039/9781849733182-00108, ISBN: 978-1-84973-002-0, 2012.

Müller, R. and Crutzen, P. J.: On the relevance of the methane oxidation cycle to "ozone hole" chemistry, in: Ozone in the troposphere and stratosphere, edited by Hudson, R. D., Proceedings of the Quadrennial Ozone Symposium 1992, pp. 298–301, 1994.

Newman, P. A., Oman, L. D., Douglass, A. R., Fleming, E. L., Frith, S. M., Hurwitz, M. M., Kawa, S. R., Jackman, C. H., Krotkov, N. A., Nash, E. R., Nielsen, J. E., Pawson, S., Stolarski, R. S., and Velders, G. J. M.: What would have happened to the ozone layer if chlorofluorocarbons (CFCs) had not been regulated?, Atmos. Chem. Phys., 9, 2113–2128, doi:10.5194/acp-9-2113-2009, 2009.

Nickolaisen, S. L., Friedl, R. R., and Sander, S. P.: Kinetics and Mechanism of the ClO+ClO Reaction – Pressure and Temperature Dependences of the Bimolecular and Termolecular Channels and Thermal-Decomposition of Chlorine Peroxide, J. Phys. Chem., 98, 155–169, 1994.

Papanastasiou, D. K., Papadimitriou, V. C., Fahey, D. W., and Burkholder, J. B.: UV Absorption Spectrum of the ClO Dimer (Cl_2O_2) between 200 and 420 nm, J. Phys. Chem. A, 113, 13 711–13 726, 2009.

Peter, T. and Grooß, J.-U.: Polar Stratospheric Clouds and Sulfate Aerosol Particles: Microphysics, Denitrification and Heterogeneous Chemistry, in: Stratospheric Ozone Depletion and Climate Change, edited by Müller, R., pp. 108–144, Royal Society of Chemistry, doi:10.1039/9781849733182-00108, ISBN: 978-1-84973-002-0, 2012.

Petzold, A., Thouret, V., Gerbig, C., Zahn, A., Brenninkmeijer, C., Gallagher, M., Hermann, M., Pontaud, M., Ziereis, H., Boulanger, D., Marshall, J., Nédélec, P., Smit, H., Friess, U., Flaud, J.-M., Wahner, A., Cammas, J.-P., and Volz-Thomas, A.: Global-scale atmosphere monitoring by in-service aircraft – current achievements and future prospects of the European Research Infrastructure IAGOS, Tellus B, 67, 28452, doi:10.3402/tellusb.v67.28452, 2015.

Plenge, J., Flesch, R., Kühl, S., Vogel, B., Müller, R., Stroh, F., and Rühl, E.: Ultraviolet Photolysis of the ClO Dimer, J. Phys. Chem., 108, 4859 – 4863, 2004.

Pope, F. D., Hansen, J. C., Bayes, K. D., Friedl, R. R., and Sander, S. P.: Ultraviolet Absorption Spectrum of Chlorine Peroxide, ClOOCl, J. Phys. Chem. A, 111, 4322–4332, doi:10.1021/jp067660w, 2007.

Prather, M. J.: More rapid ozone depletion through the reaction of HOCl with HCl on polar stratospheric clouds, Nature, 355, 534–537, 1992.

Röth, E.-P. and Ehhalt, D. H.: A simple formulation of the CH_2O photolysis quantum yields, Atmos. Chem. Phys., 15, 7195–7202, doi:10.5194/acp-15-7195-2015, 2015.

Sander, S. P., Abbatt, J., Barker, J. R., Burkholder, J. B., Friedl, R. R., Golden, D. M., Huie, R. E., Kolb, C. E., Kurylo, M. J., Moortgat, G. K., Orkin, V. L., and Wine, P. H.: Evaluation No. 17, JPL Publication 10-6, Chemical Kinetics and Photochemical Data for Use in Atmospheric Studies, Jet Propulsion Laboratory, Pasadena, 2011a.

Sander, S. P., Friedl, R. R., Barker, J. R., Golden, D. M., Kurylo, M. J., Wine, P. H., Abbatt, J. P. D., Burkholder, J. B., Kolb, C. E., Moortgat, G. K., Huie, R. E., and Orkin, V. L.: Chemical kinetics and photochemical data for use in atmospheric studies, JPL Publication 10-6, 2011b.

Santee, M. L., MacKenzie, I. A., Manney, G. L., Chipperfield, M. P., Bernath, P. F., Walker, K. A., Boone, C. D., Froidevaux, L., Livesey, N. J., and Waters, J. W.: A study of stratospheric chlorine partitioning based on new satellite measurements and modeling, J. Geophys. Res., 113, D12307, doi:10.1029/2007JD009057, 2008.

Schoeberl, M. R. and Hartmann, D. L.: The Dynamics of the Stratospheric Polar Vortex and Its Relation to Springtime Ozone Depletions, Science, 251, 46–52, 1991.

Shi, Q., Jayne, J. T., Kolb, C. E., Worsnop, D. R., and Davidovits, P.: Kinetic model for reaction of $ClONO_2$ with H_2O and HCl and HOCl with HCl in sulfuric acid solutions, J. Geophys. Res., 106, 24 259–24 274, doi:10.1029/2000JD000181, 2001.

Solomon, S.: Stratospheric ozone depletion: A review of concepts and history, Rev. Geophys., 37, 275–316, doi:10.1029/1999RG900008, 1999.

Solomon, S., Garcia, R. R., Rowland, F. S., and Wuebbles, D. J.: On the depletion of Antarctic ozone, Nature, 321, 755–758, 1986.

Solomon, S., Portmann, R. W., Sasaki, T., Hofmann, D. J., and Thompson, D. W. J.: Four decades of ozonesonde measurements over Antarctica, J. Geophys. Res., 110, D21311, doi:10.1029/2005JD005917, 2005a.

Solomon, S., Portmann, R. W., Thompson, D. W. J., Oltmans, S. J., and Thompson, A. M.: On the distribution and variability of ozone in the tropical upper troposphere: Implications for tropical deep convection and chemical-dynamical coupling, Geophys. Res. Lett., 32, doi:10.1029/2005GL024323, 2005b.

Solomon, S., Haskins, J., Ivy, D. J., and Min, F.: Fundamental differences between Arctic and Antarctic ozone depletion, Proc. Natl. Acad. Sci., 111, 6220–6225, doi:10.1073/pnas.1319307111, 2014.

Solomon, S., Kinnison, D., Bandoro, J., and Garcia, R.: Simulation of polar ozone depletion: An update, J. Geophys. Res., 120, 7958–7974, doi:10.1002/2015JD023365, 2015.

Stimpfle, R. M., Wilmouth, D. M., Salawitch, R. J., and Anderson, J. G.: First measurements of ClOOCl in the stratosphere: The coupling of ClOOCl and ClO in the Arctic polar vortex, J. Geophys. Res., 109, D03301, doi:10.1029/2003JD003811, 2004.

Stolarski, R. S., Krueger, A. J., Schoeberl, M. R., McPeters, R. D., Newman, P. A., and Alpert, J. C.: Nimbus 7 satellite measurements of the springtime Antarctic ozone decrease, Nature, 322, 808–811, 1986.

Tolbert, M. A., Rossi, M. J., and Golden, D. M.: Heterogeneous Interactions of Chlorine Nitrate, Hydrogen Chloride, and Nitric Acid with Sulfuric Acid Surfaces at Stratospheric Temperatures, Geophys. Res. Lett., 15, 847–850, 1988.

Toumi, R., Jones, R. L., and Pyle, J. A.: Stratospheric ozone depletion by $ClONO_2$ photolysis, Nature, 365, 37–39, 1993.

Tyndall, G. S., Wallington, T. J., and Ball, J. C.: FTIR Product Study of the Reactions CH_3O_2 + CH_3O_2 and CH_3O_2 + HO_2, J. Phys. Chem. A, 102, 2547–2554, 1998.

UNEP: Montreal Protocol on substances that deplete the ozone layer, United Nations Environmental Programme, Nairobi, Kenya, 1987.

von Hobe, M. and Stroh, F.: Stratospheric halogen chemistry, in: Stratospheric Ozone Depletion and Climate Change, edited by Müller, R., pp. 78–107, Royal Society of Chemistry, doi:10.1039/9781849733182-00108, ISBN: 978-1-84973-002-0, 2012.

von Hobe, M., Salawitch, R. J., Canty, T., Keller-Rudek, H., Moortgat, G. K., Grooß, J.-U., Müller, R., and Stroh, F.: Understanding the kinetics of the ClO dimer cycle, Atmos. Chem. Phys., 7, 3055–3069, 2007.

von Hobe, M., Stroh, F., Beckers, H., Benter, T., and Willner, H.: The UV/Vis absorption spectrum of matrix-isolated dichlorine peroxide, ClOOCl, Phys. Chem. Chem. Phys., 11, 1571–1580, doi:10.1039/b814373k, 2009.

WMO: Scientific assessment of ozone depletion: 2014, Global Ozone Research and Monitoring Project–Report No. 55, Geneva, Switzerland, 2014.

Zahn, A., Weppner, J., Widmann, H., Schlote-Holubek, K., Burger, B., Kühner, T., and Franke, H.: A fast and precise chemiluminescence ozone detector for eddy flux and airborne application, Atmos. Meas. Tech., 5, 363–375, doi:10.5194/amt-5-363-2012, 2012.

Zhong, W. and Haigh, J. D.: Improved Broadband Emissivity Parameterization for Water Vapor Cooling Rate Calculations, J. Atmos. Sci., 52, 124–138, 1995.

Jül-4394
Mai 2016
ISSN 0944-2952